Aarushi24pes19.pdf

Rashtriya Raksha University

Document Details

Submission ID
trn:oid:::30110:142608149

Submission Date
Jun 11, 2026, 4:09 PM GMT+5:30

Download Date
Jun 11, 2026, 4:15 PM GMT+5:30

File Name
Aarushi24pes19.pdf

File Size
2.8 MB

89 Pages

19,732 Words

112,274 Characters

3% Overall Similarity

The combined total of all matches, including overlapping sources, for each database.

Filtered from the Report

- Bibliography
- Small Matches (less than 14 words)

Match Groups

29 Not Cited or Quoted 2%
Matches with neither in-text citation nor quotation marks

0 Missing Quotations 0%
Matches that are still very similar to source material

1 Missing Citation 0%
Matches that have quotation marks, but no in-text citation

0 Cited and Quoted 0%
Matches with in-text citation present, but no quotation marks

Top Sources

1% Internet sources
0% Publications
2% Submitted works (Student Papers)

Integrity Flags

1 Integrity Flag for Review

Replaced Characters
156 suspect characters on 17 pages
Letters are swapped with similar characters from another alphabet.

Our system's algorithms look deeply at a document for any inconsistencies that would set it apart from a normal submission. If we notice something strange, we flag it for you to review.

A Flag is not necessarily an indicator of a problem. However, we'd recommend you focus your attention there for further review.

Match Groups

- **29** Not Cited or Quoted 2%
  Matches with neither in-text citation nor quotation marks
- **0** Missing Quotations 0%
  Matches that are still very similar to source material
- **1** Missing Citation 0%
  Matches that have quotation marks, but no in-text citation
- **0** Cited and Quoted 0%
  Matches with in-text citation present, but no quotation marks

Top Sources

1% Internet sources
0% Publications
2% Submitted works (Student Papers)

Top Sources

The sources with the highest number of matches within the submission. Overlapping sources will not be displayed.

1	Submitted works	Universiti Kuala Lumpur on 2026-01-19 <1%
2	Submitted works	Edith Cowan University on 2026-04-17 <1%
3	Internet	ndl.ethernet.edu.et <1%
4	Submitted works	APJ Abdul Kalam Technological University, Thiruvananthapuram on 2025-04-21 <1%
5	Submitted works	South Bank University on 2026-05-17 <1%
6	Submitted works	University of Nottingham on 2026-04-02 <1%
7	Submitted works	University of Greenwich on 2015-04-09 <1%
8	Internet	www.freepatentsonline.com <1%
9	Internet	www.mdpi.com <1%
10	Submitted works	Edith Cowan University on 2026-04-11 <1%

11 Submitted works
University of Technology, Sydney on 2026-06-06 <1%

12 Submitted works
Birla Institute of Technology and Science Pilani on 2024-06-09 <1%

13 Submitted works
University of Adelaide on 2026-05-24 <1%

14 Submitted works
Anna University on 2024-06-24 <1%

15 Submitted works
Loughborough College on 2024-05-30 <1%

16 Submitted works
University of Leeds on 2012-02-29 <1%

17 Internet
espace.curtin.edu.au <1%

18 Submitted works
AUT University on 2025-08-29 <1%

19 Submitted works
Koc University on 2025-10-29 <1%

20 Submitted works
Queen Mary and Westfield College on 2026-05-06 <1%

21 Submitted works
iGroup on 2016-07-14 <1%

22 Submitted works
Cranfield University on 2006-12-19 <1%

23 Submitted works
Delhi Technological University on 2026-06-01 <1%

24 Publication
R.M. Cuzner, D.J. Nowak, A. Bendre, G. Oriti, A.L. Julian. "Control and implementat... <1%

25 Submitted works

University of Hertfordshire on 2026-04-27 <1%

26 Submitted works

Visvesvaraya Technological University on 2014-10-29 <1%

ABSTRACT

Auxiliary systems in electric vehicles (EVs) need several regulated voltage levels for the operation of sensors, communication interfaces, embedded controllers, gate driver circuits, cooling systems, and monitoring units. Traditional auxiliary power setups typically utilize several independent DC DC converters to generate different voltage levels, leading to increased circuit complexity, switching losses, thermal stress, component count, and overall converter size. Furthermore, achieving stable regulation with separate converter stages proves challenging under changing operating conditions.

This thesis details the modelling, analysis, and closed-loop control of a Single-Input Dual-Output (SIDO) integrated DC–DC converter comprising a (NOSL-Luo Converter) combined with a Buck Converter. The topology is designed to simultaneously generate controlled positive and negative output electrical levels from a single 24 V DC input supply. The Buck converter segment delivers a regulated +12 V output ideal for low-voltage auxiliary loads, whereas the NOSL-Luo section produces a regulated −48 V output through voltage-lift techniques intended for applications that require high gain negative voltage conversion.

The converter is examined under Continuous Conduction Mode (CCM) conditions.

Mathematical modeling, operating modes, voltage transfer characteristics, ripple performance, and energy transfer principles of the proposed topology have been investigated in detail. A small-signal model and transfer functions have been derived to analyze the dynamic behavior of the converter. A closed-loop proportional-integral controller has been employed for achieving voltage stability under varying conditions of input and load. Bode plot stability analysis has been applied to the integrated circuit.

The converter circuit has been modeled using MATLAB/Simulink with similar operational parameters used to analyze the integrated converter along with the standalone ones. The results obtained show satisfactory voltage regulation, ripple control, steady-state response, and dual output power supply operation of the circuit. It is seen that the use of integrated circuits decreases the need of having different converters and improves its efficiency.

It can be concluded from the discussion above that the integration of the Buck Converter circuit along with the Negative Output Super-Lift Luo Converter provides an efficient and compact way of supplying low-power EV auxiliary systems with two voltage supplies from a common DC supply.

Keywords: Integrated Dc-Dc Converter, Negative Output Super-Lift Luo Converter, Buck Converter, Dual Output Converter, Voltage Lift Circuit, EV Auxiliary Systems.

G(s)	Transfer function
(s)	Laplace operator
Kp	Proportional gain
Ki	Integral gain
Vref	Reference voltage
d(t)	Small signal duty perturbation
$\hat{v}$	Small signal voltage variation
$\hat{\imath}$	Small signal current variation
Q	MOSFET switch
(D_1, D_2, D_3)	Diodes
t_{on}	Switch ON duration
t_{off}	Switch OFF duration
E_L	Energy stored in inductor
E_C	Energy stored in capacitor
P_{out}	Output Power
$P_{Load\ 1}$	Luo load power
P_{Load2}	Buck Load Power

turnitin Page 7 of 94 - Integrity Submission Submission ID trn:oid:::30110:142608149

CHAPTER 1
INTRODUCTION

1.1 Evolution of Electric Vehicle Power Systems

With the development of EVs, there is a huge need for efficient and reliable power electronic converters. EVs have been developed with a number of auxiliary systems besides the traction drives. These systems include battery management systems, controllers, sensors, communication links, entertainment systems, thermal regulation systems, lighting systems, dashboards, and monitoring and protective circuits. As these components use power at various voltages, the voltage generated by the main battery in EVs cannot be applied directly to all these loads. Efficient DC-DC converters have therefore become necessary for such systems.

A number of low-powered auxiliary loads including sensors, relays, microcontrollers, cooling systems, lighting systems, and controls systems require a steady power supply of 12 V DC. On the other hand, some communication interfaces, telecommunication systems, gate drivers, and signal conditioning devices require a negative power supply like -48V. Due to the wide range of voltage requirements, a power electronic converter that can produce positive as well as negative outputs using the same power source would prove very useful.

Traditional converter techniques including the Buck, Boost, Buck-Boost, Ćuk, and SEPIc converters have been extensively employed in voltage conversion systems. However, in the case of multiple output voltages, individual converters are required to be designed. Hence, this approach would increase the total number of components, increase circuitry complexity, switching losses, increase the converter physical size, and hence, system costs. Utilizing multiple independent converters increases losses due to their conduction and switching losses; thus, reducing efficiency.

Another key drawback associated with traditional converter configurations includes large output voltage ripple and low efficiencies at high switching frequencies. High output voltage ripple adversely affects load performance since the load requires low-ripple outputs. Moreover, the switching losses create thermal stresses that lead to reduced efficiency and increased complexity for controlling the converter.

In order to solve the problems above, integrated dual output converter structures have been gaining interest lately. Converters can produce different types of output voltages with the same switching configuration. It is an effective way to lower the number of components used, achieve better power density, minimize energy loss, and optimize the efficiency of a particular system. The use of an integrated converter is much better suited to the needs of EV auxiliary power systems.

In regard to various topologies of DC-DC converters with high gain, there is a topology called Negative Output Super-Lift Luo Converter. When integrated with a Step-Down (Buck) Converter, the combined topology can simultaneously generate a regulated positive output voltage and a high-magnitude negative output voltage from a single DC input source. This makes the converter highly suitable for EV auxiliary systems requiring both +12 V and −48 V supplies.

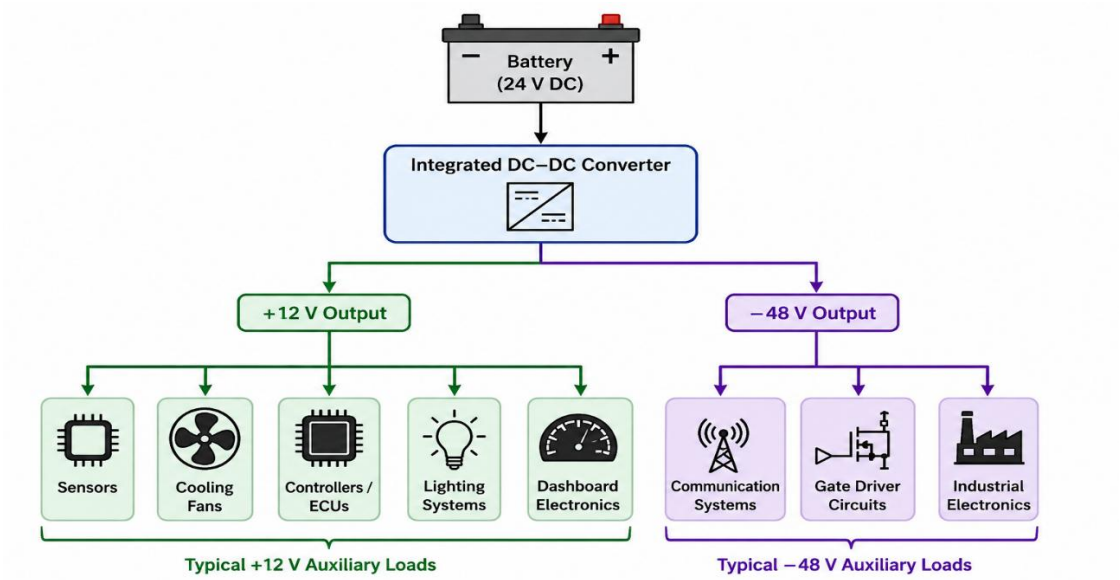

Figure 1.1: Typical Auxiliary Power Distribution in Electric Vehicle

In this work, a Negative Output Super-Lift Luo Converter integrated with a Buck Converter is designed and analysed for a 24 V DC input supply. The integrated converter generates regulated output voltages of +12 V and −48 V simultaneously. Closed-loop control is implemented to achieve stable voltage regulation under varying input conditions. The overall performance of the converter is evaluated through detailed simulation studies including voltage regulation analysis, efficiency evaluation, transfer function analysis, small-signal modelling, bode plot analysis, and energy storage analysis of passive components.

1.2 Role of DC–DC Converters in EV Applications

DC–DC converters are an important part of modern electric vehicle (EV) power systems. These converters are used to convert one level of DC voltage into another regulated DC voltage according to the requirements of different electronic subsystems present in the vehicle. For this reason, DC–DC converters can be used in order to give proper voltages for various devices which run on different voltages within an EV since the voltage level from the EV battery cannot meet the requirements of all devices.

For example, various auxiliary systems in EVs such as sensors, embedded controllers, battery management system (BMS), cooling fan system, instrument cluster electronics, communication systems, and infotainment system are mostly supplied with relatively lower voltage level such as +12V. Moreover, some communication systems, gate drivers, and industrial electronics need negative voltage such as −48V.

As a result, a multi-voltage converter is necessary in order to supply those auxiliary systems with a sufficient amount of voltage and current. The performance of the auxiliary power system largely depends on the performance of the DC–DC converter. Such parameters as voltage regulation, switching characteristics, output ripple, transient response, power density, and heat performance are especially significant. Different converters are used for various purposes, and these are the Buck, Boost, Buck-Boost, Ćuk, SEPIC, and Luo converters.

The most popular topology among those is the Buck converter, since this topology can be easily used in order to achieve a desired low-voltage output. However, standard converters cannot operate effectively in case of necessity to achieve a relatively large voltage gain or negative polarity output.

The NOSL Luo converter offers better voltage gain performance and boost performance than traditional converters. Using the concept of voltage lift, the converter is able to provide better negative output voltage performance with more gains, making it appropriate for use in EV auxiliary circuits that require negative output voltages.

Converter	Conversion Type	Gain	Polarity	Key Advantage	Major Limitation
Buck	Step-down	Low	Positive	High efficiency and simple control	Cannot provide voltage boost
Boost	Step-up	Moderate	Positive	Simple voltage boosting	High ripple and switch stress
Buck–Boost	Step-up / Step-down	Moderate	Negative	Wide voltage conversion range	Higher switching stress
Ćuk	Step-up / Step-down	Moderate	Negative	Low input/output ripple	More passive components
SEPIC	Step-up / Step-down	Moderate	Positive	Non-inverted output	Lower efficiency at high gain
Negative Output Super-Lift Luo	High-gain Step-up	High	Negative	High voltage gain with improved boosting	Complex control and design

Table 1.1 Comparison of Common DC–DC Converter Topologies for EV Applications

1.3 Limitations of Conventional Converter Systems

Whereas conventional EV auxiliary power supplies rely on multiple DC-to-DC converters to provide various voltages according to each electronic sub-system, a common practice is that a buck converter may be used to regulate +12 V voltage to drive a low-voltage device, whereas a second independent inverter must be provided to generate negative voltages necessary for communication ports, gate drivers, and electronics.

Whereas this strategy successfully caters to voltage generation, there are certain drawbacks associated with the strategy mentioned above.

1. Increased Circuit Complexity and Component Count

Use of individual converter sections will need a greater number of power semiconductors, inductors, capacitors, gate drives, and controllers, thus making the overall system bulky. Increase in hardware components makes the system complicated. This factor directly impacts the size of the system, and system size is a significant factor in the design of EV systems.

2. Higher Switching and Conduction Losses

As all converters operate independently with their unique switches, repetitive switching results in higher switching loss and conduction loss. The loss lowers the efficiency of conversion of power and leads to unnecessary losses of power.

3. Increased Output Voltage and Current Ripple

Several conversions lead to additional ripples of voltage and current. Ripple that is too high might affect delicate electronic circuitry like sensors, communication devices, microcontrollers, and control circuits, thus reducing system efficiency and power quality.

4. Reduced Overall System Efficiency

In a traditional system where several converters are used, the electrical energy is made to pass through different channels for conversion, thus increasing the total losses. Therefore, the efficiency of the auxiliary power system is greatly reduced.

5. Complex Control and Regulation

Stable operation in multiple converters requires different closed loop control designs and control schemes that will complicate the process of designing the controllers and integrate them into one system especially when fast dynamic performance is required.

6. Increased Thermal Stress and Reduced Reliability

Further, additional switching elements as well as passive elements lead to higher thermal stress as power loss is increased. The effect of excessive heat generation is that it reduces

the reliability of the converter, reduces the lifespan of components and calls for further cooling methods, which will add up to the costs involved. Such limitations highlight the need for a converter architecture that can provide more than one regulated output using a common power conversion system.

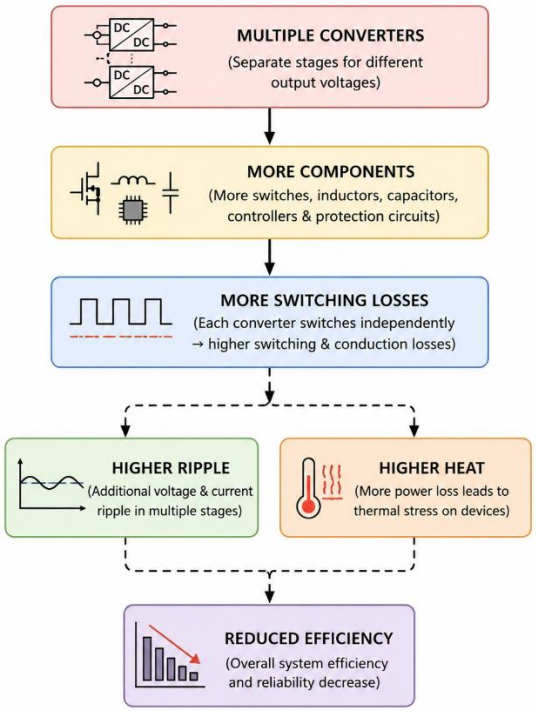

Figure 1.2 Problems in Conventional Multi-Converter Architecture

1.4 Need for Integrated Dual-Output Converter

Dual-output converter integrated architectures have become an area of great interest to researchers nowadays due to the weaknesses that come with using conventional converter architectures. Instead of having multiple converters, the architecture involves a single switching circuit that simultaneously produces several different outputs, minimizing hardware and improving energy consumption.

The architecture consists of:

- a Buck converter for the +12 V output and
- the Negative Output Super-Lift Luo Converter for the −48 V output.

What's more, the architecture facilitates the generation of both outputs using only one 24 V DC input. Some of the benefits of this converter model include:

- Compact architecture,
- Fewer switching components,
- Better voltage gain,
- Less loss,

- ❖ Higher efficiency,
- ❖ Cost minimization, and
- ❖ Easier power management.

Overall, this makes the converter very efficient and appropriate for auxiliary electric vehicles.

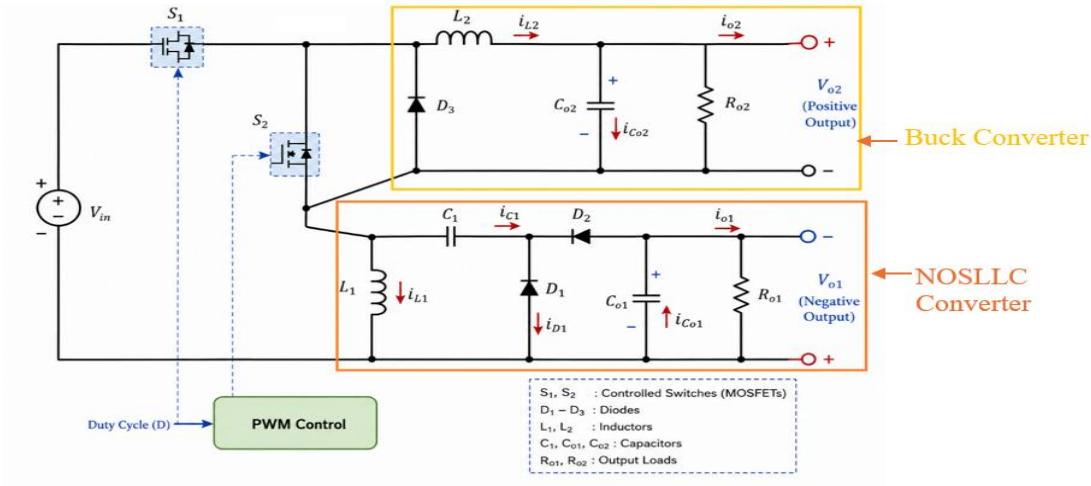

Figure 1.3 Negative output self-lift Luo Converter integrated with buck converter

1.5 Motivation of the Work

This progress in technology has led to an increased need for effective and efficient power converters, which can provide multiple voltage levels from one converter to drive various electronics. In practical applications, there are different subsystems in the EV that require different voltages for their proper operation. Using converters for different voltages would increase the complexity of circuits, as well as the cost of implementation due to increased number of components and switching losses. Conventional converters have less efficient utilization of power since they use multiple switches, as well as multiple components for regulation of the desired output. The more converter stages are used, the more difficult the design of the converter becomes. The aim of the integrated converter is to provide a solution to these problems.

The major motivations behind this work are:

- ❖ To generate both positive and negative regulated output voltages from a single DC input source
- ❖ To reduce the number of power switches and passive components compared to conventional multi-converter systems

- To achieve a more compact and simplified converter structure suitable for EV auxiliary applications
- To improve voltage, gain capability using the Negative Output Super-Lift Luo Converter topology
- To reduce switching losses and improve overall power conversion efficiency
- To provide a regulated +12 V output for low-voltage auxiliary loads such as sensors, controllers, and monitoring circuits
- To generate a −48 V output suitable for communication interfaces and gate driver applications
- To improve utilization of the available input power source through an integrated conversion approach
- To implement closed-loop control for improved voltage regulation and stable converter operation
- The work therefore focuses on developing a practical and efficient dual-output converter topology that combines compact design, improved voltage gain characteristics, and reliable output regulation for EV auxiliary power systems.

Parameter	Conventional System	Integrated Converter
Converter Structure	Multiple converters	Single integrated topology
Switching Devices	Higher count	Reduced count
Control Scheme	Multiple controllers	Common control structure
Switching Losses	Higher	Reduced
Output Ripple	Higher	Lower
Voltage Gain	Moderate	High
Efficiency	Lower	Improved
Thermal Stress	Higher	Reduced
Power Density	Lower	Higher
Size and Cost	Bulky and costly	Compact and economical
EV Application Suitability	Limited	More suitable for auxiliary systems

Table 1.2 Comparison Between Conventional and Integrated System

1.6 Objectives of the Thesis

1. Goals and aims of this investigation are as follows:
2.
3. 1. To develop a complete mathematical model of the hybrid Luo Converter along with the Buck Converter for application in EV auxiliaries.

4. 2. To generate dual regulated output voltages of +12V and -48V from an input supply of 24V DC.
5. 3. To use closed-loop control for ensuring stable voltage regulation.
6. 4. To test the converter performance at different values of input voltages.
7. 5. To undertake small-signal analysis and derive the transfer function of the complete hybrid circuit.
8. To analyse converter stability using bode plot analysis.
9. To evaluate converter performance through:

    - ❖ Input power analysis
    - ❖ Output power analysis
    - ❖ Efficiency analysis
    - ❖ Inductor energy storage analysis
    - ❖ Capacitor energy storage analysis

10. To compare the performance advantages of the integrated converter over conventional converter structures.

1.7 Scope of the Work

The present work focuses on the simulation-based modelling, analysis, and closed-loop control of the integrated dual-output converter topology for EV auxiliary applications.

The scope of the work includes:

- ❖ converter operation and performance analysis,
- ❖ closed-loop control implementation,
- ❖ small-signal modelling and transfer function analysis,
- ❖ stability analysis using bode plots,
- ❖ efficiency and power flow evaluation,
- ❖ and energy storage analysis of inductive and capacitive elements.

The study is carried out using MATLAB/Simulink environment and is limited to simulation analysis

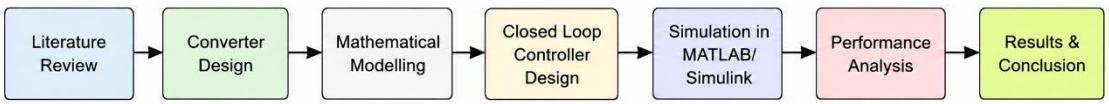

Figure 1.4 Workflow of the Present Study

17

1.8 Organization of the Dissertation

The dissertation is organized into the following chapters:

Chapter 1 – Introduction

This chapter presents the background of electric vehicle (EV) auxiliary power systems and highlights the importance of DC–DC converters in EV applications. It discusses the limitations of conventional converter topologies, the need for integrated dual-output converters, the motivation behind the proposed work, and the objectives and scope of the dissertation.

Chapter 2 – Literature Review

This chapter reviews the existing research on conventional DC–DC converters, Luo converter topologies, integrated multi-output converter structures, and control techniques. It identifies the research gap and establishes the motivation for developing the proposed integrated converter topology.

Chapter 3 – Analysis of Individual Converter Topologies

This chapter investigates the operating principles and performance characteristics of the Buck converter and the Negative Output Super-Lift (NOSL) Luo converter independently. The converter operation, voltage conversion relationships, closed-loop control structures, simulation parameters, and performance analyses are presented. A comparative analysis is also carried out to highlight the need for an integrated converter configuration.

Chapter 4 – Integrated Buck–NOSL Luo Converter Topology and Operation

This chapter introduces the proposed integrated converter topology and explains its circuit configuration, power flow mechanism, voltage-lift operation, and switching modes. Detailed mode-wise analysis and voltage gain derivation are presented, followed by the design specifications and closed-loop control structure of the integrated converter.

Chapter 5 – Mathematical Modelling and Stability Analysis

This chapter presents the mathematical modelling of the proposed integrated converter using state-space techniques. State variable selection, state-space averaging, small-signal modelling, transfer function derivation, PI controller design, and stability evaluation through frequency-domain analysis are discussed in detail.

Chapter 6 – Performance Analysis of the Converter

This chapter presents the MATLAB/Simulink-based performance evaluation of the proposed converter. The analysis includes input and output voltage responses, power flow

characteristics, efficiency analysis, switching waveform analysis, and energy transfer performance under closed-loop operation.

Chapter 7 – Conclusion and Future Scope

This chapter provides a summary of the important findings from the research conducted. The efficiency of the newly developed combined converter configuration is stressed while outlining possible areas for future research to improve the performance of this approach.

CHAPTER 2
LITERATURE REVIEW

Compactness and efficient DC-DC converters with the ability to produce different voltages with minimized switching losses and better voltage regulation are required for electric vehicles auxiliary systems. Today, various voltage supplies are needed for auxiliary equipment including controllers, sensors, lighting units, embedded electronics, and battery management systems. Consequently, there has been a significant rise in the demand for efficient, compact, less rippled, and better regulated voltage supply using converter topologies.

Recent investigations include the implementation of multi-output converter topologies, voltage-lift technology, and combined topologies for improved converter operation with fewer switching losses and decreased complexities. Among all converter topologies, Luo converters gained much popularity due to their potential for higher voltage conversion, low rippling, and simple design. The voltage lift property makes Luo converter topology preferable when it comes to designing more voltage conversion-efficient applications.

This chapter highlights a review of literature pertinent to Luo converters, combined DC-DC converters, voltage-lift methods, and multi-output converters for EV applications, all of which are relevant to the proposed converter system architecture.

2.1 Review of Conventional DC–DC Converter Topologies

To convert and regulate the voltage, the electric vehicle auxiliary system has been widely using various DC-DC converters. In previous works researchers are trying to develop such converter topologies (Buck, Boost, Buck-Boost, uk and Single-Inductor Multi-Output converter) to improve the converter efficiency, minimize the switching losses and to decrease the complexity of converter. The recent researchers are more concentrate to the compact converter topologies and generating multiple outputs with less number of switches and passive component.

In order to reduce the number of magnetic components, the size and the cost of the converter Chen et al developed systematic derivation technique for the Single-Inductor Multi-Input Multi-Output (SI-MIMO) DC-DC converter structures. The developed

converter topologies utilize a single inductor among the different input and output ports to improve the efficiency, reduce the component size, number of components and the total system cost. Different converter topologies have been derived by combining the Buck, Boost and Buck-Boost converter topologies and the behavior of converter such as Continuous Conduction Mode (CCM) and Discontinuous Conduction Mode (DCM) operations has been described in detail. The authors confirmed that the developed multi-output structures will be beneficial for the electric vehicles and other systems requiring less amount of compact and effective DC-DC converters.

In order to generate the step-up and step-down outputs simultaneously with the same switching structure Faridpak et al suggested an integrated structure, a Super-Lift Luo Converter combined with a Buck Converter to improve voltage gain capability, decrease the output ripple and reduction of switching loss. This type of integrated structure had verified using MATLAB/Simulink and experimental result at various operation conditions.

It is observed from the review of the various researches that integrated converter structures were most beneficial for the EV auxiliary applications which were having more than one voltage requirement.

S. No	Research Work	Converter Topology	Major Contribution	Application Area	Important Observations
1	Chen et al.	SI-MIMO DC–DC Converter	Systematic derivation of multi-input multi-output converter structures using single inductor	EVs, renewable systems	Reduced magnetic components and compact converter structure
2	Faridpak et al.	Super-Lift Luo integrated with Buck Converter	Simultaneous step-up and step-down operation using integrated topology	EV auxiliary systems	Improved voltage gains and reduced switching losses

Table 2.1 Review of Conventional DC–DC Converter Topologies

2.2 Review of Luo Converter Topologies

Luo converters have gained a lot of interest due to its voltage-lift capability, better voltage transfer gain and suitability for high gain applications. Elementary Lift Luo Converter, Self-Lift Luo Converter and Super-Lift Luo Converter are different forms of Luo converter which have been analyzed for various application such as renewable energy system, auxiliary application for EV's and regulated power supply.

Binitta Robin et al. Proposed an Improved Negative Output Super-Lift Luo Converter (INOSLC) which used PI controller for better regulated output voltage and higher voltage gain. The converter utilized the voltage lift method to achieve better voltage transfer characteristics with low ripple contents. Detailed operating modes and the modeling and controller were also shown using analysis with MATLAB/Simulink. The article showed the stability of the converter under changing condition when control is used in close loop. Saja Salim Ali et al. Presented review and comparison of different topologies of Negative Output Luo Converter. Their working principles, characteristics of voltage gain, performance of ripples and the control method are being shown. Also it has shown that the control of the Luo converter structures such as PI controller, PID controller, fuzzy logic controller, sliding mode controller is evaluated in each of the topologies. This article emphasized the Super-Lift Luo converter topologies which give higher voltage gain and good regulation characteristics.

It has been shown in literature reviewed that the Luo converter topologies is very suitable for applications which require higher voltage gain with less ripple and efficiency is improved. Voltage-lift property of Luo converters make them suitable for integrated converter with high gain voltage conversion.

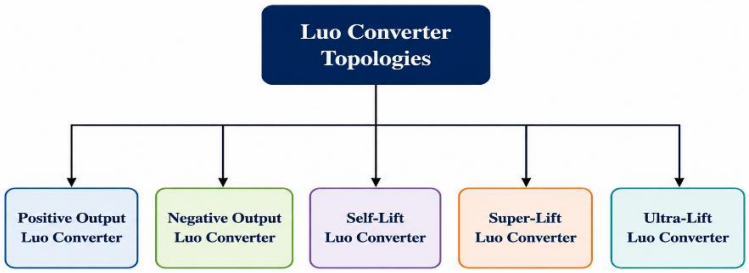

Figure 2.1 Classification Diagram of Luo Converters

S. No.	Research Work	Converter Topology	Major Contribution	Control Method	Important Observations
1	Binitta Robin et al.	Improved Negative Output Super-Lift Luo Converter	Higher voltage gain and improved regulation using voltage-lift technique	PI Control	Stable closed-loop operation and reduced ripple
2	Saja Salim Ali et al.	Review of Negative Output Luo Converters	Comparative study of various Luo converter structures	PI, PID, Fuzzy, Sliding Mode	Super-Lift Luo topology provides improved gain characteristics

Table 2.2 Review of Luo Converter Topologies

2.3 Review of Integrated Multi-Output Converter Systems

The research on integrated multi-output converters has gained much attention, as space and efficiency are highly desirable for EV auxiliary systems. These converter topologies use a common switching structure and a common magnetic structure to realize two or more regulated DC outputs.

Ghasemi et al. Developed a single-switch multi-output converter which integrates Luo topology with coupled inductor and flyback converters. Multiple step-up outputs were derived from a single input with a single active switch. The developed converter also exhibits improved voltage gain and lower switching stress; better utilization of magnetic components. This paper also elaborated on the methods to recycle the energy in order to enhance converter efficiency, minimize EMI and hence develop efficient converter.

Vennila et al. Proposed a Negative Output Super-Lift Luo Converter with a Step-Down Converter to be used in EV battery charging and auxiliary systems. It is a Single-Input Dual-Output (SIDO) converter and develops two simultaneously present high gain negative output and regulated low voltage output from a single DC input. They also present the mathematical modeling, switching mode analysis and simulations in MATLAB/Simulink under different duty ratios.

It can be seen from the reviewed integrated converters, combination of a high-gain converter and low-voltage auxiliary supply converter is required in the integrated configuration to achieve high degree of miniaturization, efficiency and improved power managing ability for EV applications.

S. No.	Research Work	Integrated Topology	Major Contribution	Output Configuration	Important Observations
1	Ghasemi et al.	Luo Converter based Multi-Output Converter	Multiple outputs using single-switch topology	Multi-output step-up	Improved gain and reduced switching stress
2	Vennila et al.	NOSL Luo integrated with Step-Down Converter	Simultaneous high-gain and low-voltage output generation	Dual-output	Suitable for EV auxiliary applications

Table 2.3 Review of Integrated Multi-Output Converter Systems

2.4 Research Gap and Motivation

With the ever-increasing number of usage of the electric vehicles, the necessity for highly compact and reliable, efficient auxiliary power conversion system that can provide multiple regulated dc outputs has increased. As seen from various research works cited above, various techniques of standalone dc-dc converters, Luo converters, multiple output converters, integrated converters are studied for applications in electric vehicles, renewable energies.

It is observed from the literature that conventionally, dc-dc converters such as Buck, Boost, Buck-Boost, Luo can achieve regulated dc voltage with quite decent steady-state performance. The Luo converter structures, due to its voltage transfer characteristics with voltage-lift method, has presented good voltage transfer ratio, ripples and is useful for high-gain conversion requirement.

Many researchers have developed integrated converter structures in order to reduce the components, overall size and switching losses in multi output converters while providing multiple outputs from the single DC source. These integrated structures are suitable for EV auxiliary system due to their need for compact size, efficiency and stable output regulation.

From the literature it is found that the Negative Output Super-Lift Luo Converter along with the step down structures is efficient for having high gain negative output voltage and the low voltage regulated outputs can also be simultaneously achieved with an effective technique. Such a system would be ideal for EV auxiliary power system that will be needed for the controller, communication systems, gate driver circuits, sensors and monitoring circuitry.

Some of the crucial information such as converter operation, voltage lift techniques, switching waveforms and its properties, mathematical model and closed-loop control strategies are gathered from various relevant literatures mentioned above. Information like the ripples of the converter, its output regulation, and the switching stresses were gathered.

Inspired by these various literature, the current investigation aims at analysis of Buck Converter and Negative Output Super-Lift Luo Converter and their integrated operation via the help of adjusted operating values and by using closed loop control and hence analyzing converter parameters and its response along with transient response, ripple

parameters, duty ratio characteristics, settling times, MOSFET switching stresses and the general performance.

The analysis performed in this work helps to comprehend the feasibility of an integrated converter structure for achieving the dual regulated outputs by a single DC source under steady closed-loop operation.

CHAPTER 3
ANALYSIS OF INDIVIDUAL CONVERTER TOPOLOGIES

3.1 Buck Converter

3.1.1 Introduction to Buck Converter

The Buck converter is one of the most widely used DC–DC converter topologies for regulated low-voltage applications. It operates as a step-down converter capable of converting a higher DC input voltage into a lower regulated DC output voltage with high efficiency and comparatively simple circuit structure. Due to its reliable operation and good voltage regulation capability, the Buck converter is extensively used in electric vehicle auxiliary systems, embedded electronic systems, battery-operated equipment, and power management applications.

Auxiliary electronic circuits in today's EV's needs regulated DC supply with low voltage for operation. They are battery monitoring systems, sensors, dashboard components, communication modules, cooling fan, relays, and some control circuits. In EV application usually, regulated +12V is necessary to power up these low power electronic loads. But the voltage from main battery can not supply to all these loads, hence it is a good candidate to use a Buck converter for regulation of output low voltage.

In the present work analysis on the buck converter individually is carried out before analyzing the entire integrated converter. The goal of this analysis is to learn about the converter switching behavior, the voltage regulation capability of the Buck converter, the transient response, ripple behavior and performance under closed-loop control. The understanding of individual buck converter enables to understand the low voltage output side of integrated converter to be analyzed later.

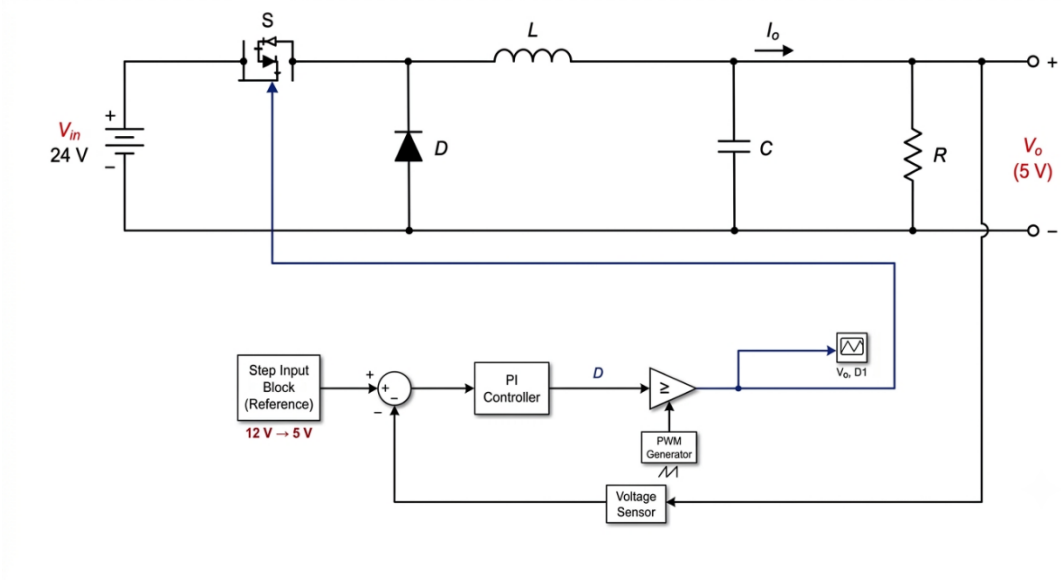

Figure 3.1 Closed-Loop Buck Converter Circuit

Figure 3.1 displays theMATLAB/Simulinkmodel that has been designed in this project for the closed-loop Buck converter. It primarily includes DC voltage source, MOSFET, freewheeling diode, inductor, output capacitor, resistive load, PWM generation circuit and the sensed parameters used to regulate the output voltage by a closed loop system which incorporates the PI controller. TheMOSFETis considered as the main switching element in the converter which is operated using the PWM signal from the control system. In the "on-state" the input voltage source transfers the energy to the inductor to be stored as magnetic energy. During the "off-state" the stored energy in the inductor is delivered to the output through freewheeling diode and it keeps on sending current to the load. Inductor and output capacitor are the components that constitute the filtering circuitry of the converter. This filtering section ensures the minimization of current and voltage ripples and regulation of the output DC voltage. The resistive load can be seen as the supplementary load the converter is supplying power. Voltage and current measurement blocks are provided so that, during the simulation process parameters of the converter like MOSFET voltage and current, inductor current, load current and output voltage can be clearly seen. In this project a close loop strategy has been employed for regulation of the output DC voltage for steady-state and transient conditions of the system by using aPI controllerwhich compares the sensed output voltage to a set point. It then provides a signal which can be used to alter the duty cycle to meet the set point. PWM signal to the gate terminal of MOSFET can be generated by comparing output of PI controller with a high frequency triangular carrier waveform. As the duty cycle is kept under regulation the

output voltage is controlled under varied circumstances and better voltage regulation performance compared to other control schemes used in the Buck converter. The simulation of the Buck converter is carried out in continuous conduction mode using the power Gui continuous solver configuration ofMATLAB/Simulink.

3.1.2 Operating Principle of Buck Converter

The operation of the Buck converter is based on the controlled switching action of the MOSFET, which alternates between ON-state and OFF-state conditions at a high switching frequency. During each switching cycle, energy is transferred from the input source to the load through the inductor and output filter network. Depending upon the switching condition of the MOSFET, the converter operation can be divided into two modes.

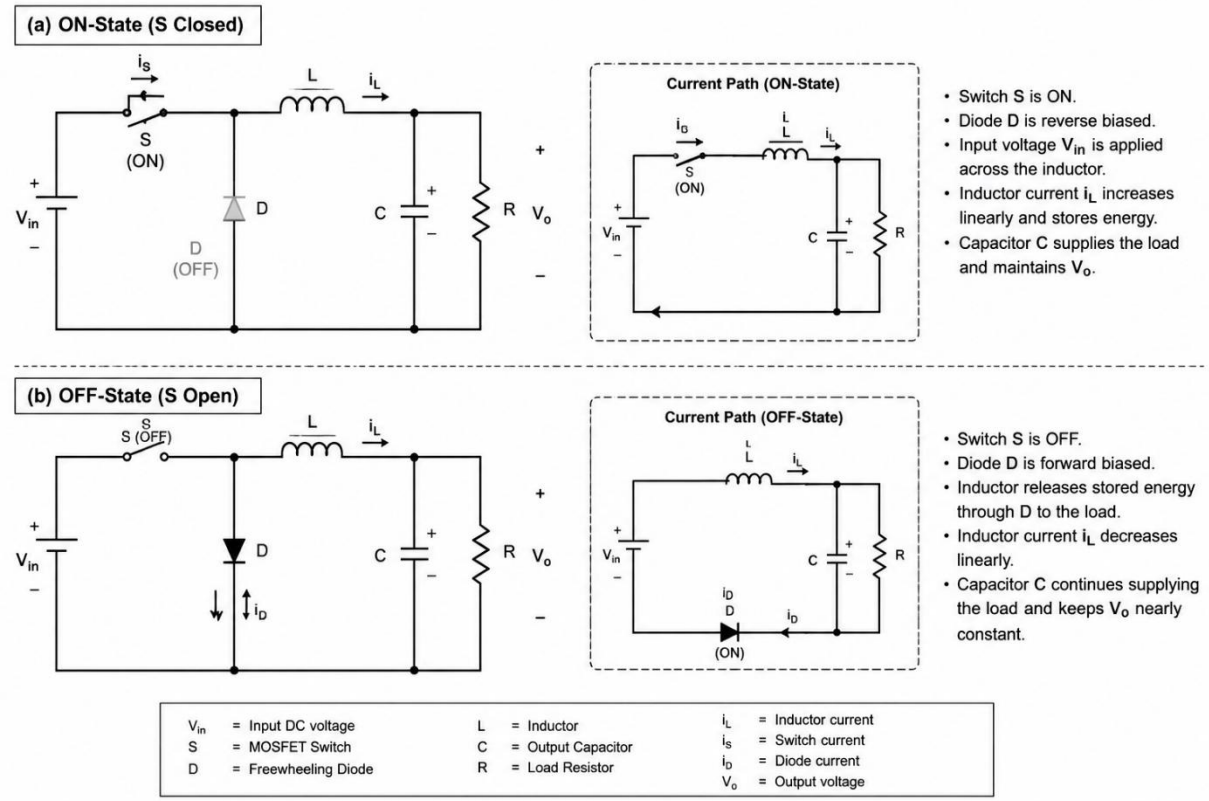

Figure 3.2 Switching Operation of Buck Converter

I. Mode 1: ON-State Operation (Switch Closed)

During Mode 1, the MOSFET switch (S) is turned ON by the PWM control signal, while the freewheeling diode (D) remains reverse biased. Under this condition, the input voltage V_{in} is directly applied across the inductor and load circuit.

The current path during this interval is:

$$\mathbf{V_{in} \rightarrow MOSFET \rightarrow Inductor \rightarrow Load \rightarrow Ground}$$

As the MOSFET conducts, the inductor current i_L increases linearly due to the positive voltage developed across the inductor. The inductor stores energy in the form of a magnetic field according to:

$$\mathbf{V_L = L\frac{diL}{dT}}$$

Since the diode is reverse biased, it does not participate in conduction during this interval. The output capacitor (C) charges and assists in maintaining a smooth output voltage across the load. The capacitor also helps reduce output voltage ripple caused by switching action.

During ON-state operation:

- MOSFET conducts current.
- Diode remains reverse biased.
- Inductor stores magnetic energy.
- Inductor current increases linearly.
- Energy is transferred from source to load.
- Capacitor supports output voltage regulation.

II. Mode 2: OFF-State Operation (Switch Open)

During Mode 2, the MOSFET switch (S) is turned OFF. Due to the sudden interruption of the main current path, the inductor opposes the change in current by reversing its polarity. This reversal forward biases the freewheeling diode (D), thereby providing an alternate path for the inductor current.

The current path during OFF-state becomes:

$$\mathbf{Inductor \rightarrow Diode \rightarrow Load \rightarrow Ground}$$

11 During this interval, the energy stored in the inductor is released to the load and output capacitor. Linear decline of the inductor current; Under the continuous conduction mode (CCM), the inductor current will never reach zero.

The relation between the declining inductor current and the time is given by:

$$\mathbf{\frac{diL}{dT} = \frac{V_L}{L}}$$

Where the inductor voltage is negative during the OFF period.

The energy for the load is supplied by the output capacitor, the output voltage is kept almost constant while switching.

During OFF-state operation:

- MOSFET remains non-conducting.
- Diode becomes forward biased.
- Inductor releases stored energy.
- Inductor current decreases linearly.
- Capacitor maintains output voltage stability.
- Load receives energy from the inductor and capacitor.

3.1.3 Output Voltage Relation of Buck Converter

The mean output voltage of the Buck converter is proportional to the duty ratio of the switching signal and under ideal operation this may be expressed as:

$$\mathbf{V_o = DV_{in}}$$

where:

- V_o = Output voltage
- V_{in} = Input voltage
- D = Duty ratio of the PWM signal

It can be observed from the relation that the output voltage of the converter can be controlled by varying the duty ratio of the switching pulses. As the duty ratio is increased the average output voltage is increased while it decreases when the duty ratio is decreased. Thus, the regulated operation of the converter under varying load conditions and supply voltages depends on accurately regulating the duty ratio.

In a closed-loop Buck converter, the PI controller adjusts the duty ratio on continuous basis depending on the difference between the reference voltage and sensed output voltage.

3.1.4 Closed-Loop Control of Buck Converter

Closed-loop control is implemented to maintain stable output voltage despite variations in operating conditions. As in case of open-loop operation, the output voltage fluctuates when the input voltage or load is perturbed. Thus, feedback is required to regulate the converter.

In this work a PI controller is employed to regulate the output voltage in closed-loop operation. The output voltage is compared with reference voltage and error signal is processed in PI controller.

Error signal is defined as:

$$\mathbf{e(t) = Vref - Vo(t)}$$

PI controller adjusts the PWM duty ratio by the error signal to keep the desired output voltage. Transient response gets better, steady state error is reduced, voltage regulation is promoted.

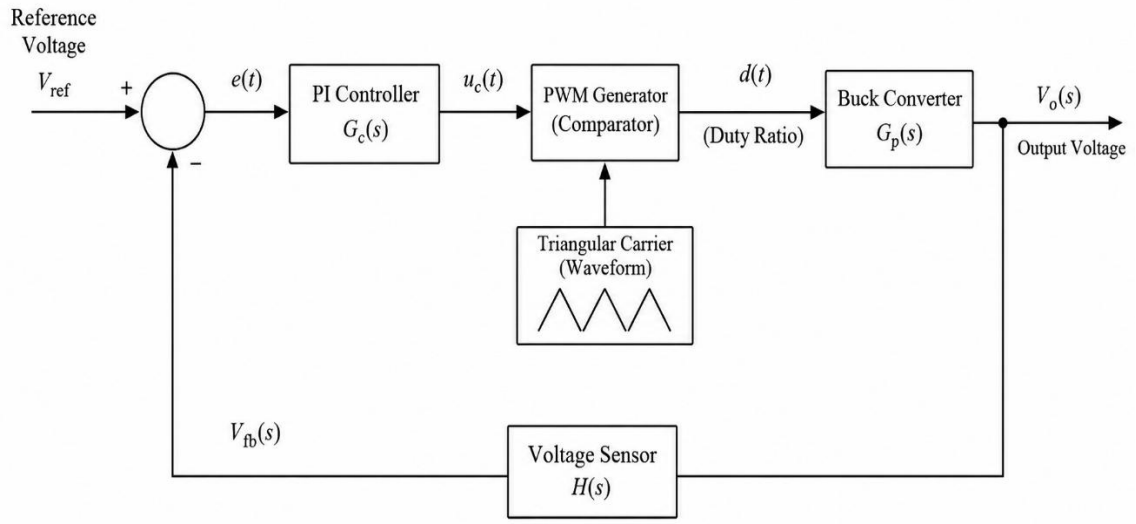

Figure 3.3 Closed-Loop Control Structure of Buck Converter

3.1.5 Simulation Parameters of Buck Converter

The stand-alone Buck converter model has been simulated in MATLAB/Simulink using the same circuit parameters as in the integrated converter topology in order to study the stand-alone closed-loop characteristics.

Parameter	Value
Input Voltage	24 V
Output Voltage	12 V
Inductance	360 µH
Capacitance	870 µF
Load Resistance	1.45 Ω
Switching Frequency	20 kHz
Controller	PI Controller

Table 3.1Simulation Parameters of Buck Converter

3.1.6 Performance Analysis of Buck Converter

In this part the behavior of the Buck converter for its transient and steady state conditions is studied by considering the output voltage regulation, inductor current waveform, MOSFET switching waveform and duty cycle behavior based on the simulation outputs.

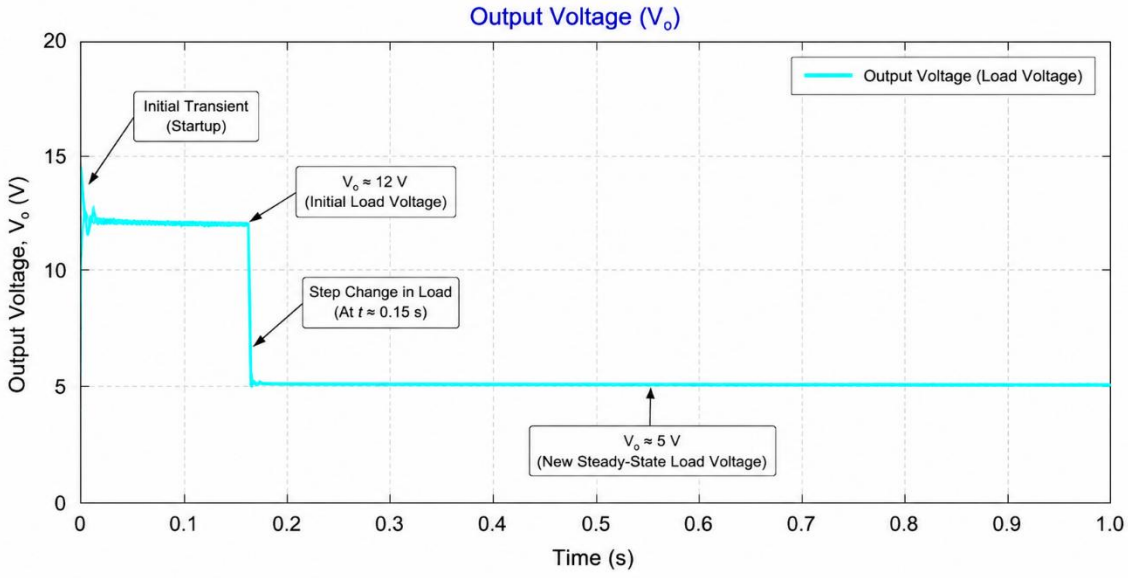

Figure 3.4Output Voltage Waveform of Buck Converter

The output voltage waveform clearly displays excellent closed loop voltage regulation. The output ripple is low and the transient response is satisfactory. During a change of reference, the output voltage of the converter follows the reference and reaches its steady state after a small transient. This waveform shows that voltage regulation can be achieved and that the closed loop operation of the converter is stable.

The ripple voltage output is evaluated:

$$\mathbf{\Delta Vo = Vo(max) - Vo(min)}$$

$$\mathrm{Vo(max)= 5.318v}$$

$$\mathrm{Vo(min) = 5.313v}$$

$$\mathbf{\Delta Vo = \sim 5mV}$$

The resulting ripple voltage is far less than the regulated output voltage, so this implies that the filteration is well and closed-loop Buck converter steady-state response is stable, voltage regulation is acceptable and output voltage is almost stable with negligible fluctuations.

The response of settling time from the step response of closed-loop Buck converter is approximately 7-8ms which indicates that the transient response and closed-loop performance is good.

The percentage overshoot of output voltage can be expressed by:

$$\%\mathbf{OS} = \frac{\mathbf{Vpeak} - \mathbf{Vfinal}}{\mathbf{Vfinal}} \times \mathbf{100}$$

Substituting the measured values:

$$\text{Vpeak} = 5.7\ \text{V}$$

$$\text{Vfinal} = 5.3\ \text{V}$$

Therefore,

$$\%\mathbf{OS} = \frac{\mathbf{5.7} - \mathbf{5.3}}{\mathbf{5.3}} \times \mathbf{100} \approx \mathbf{7.54}\%.$$

The overshoot obtained from the analysis of Buck converter. It clearly show that the converter reaches to steady state voltage with allowable transient deviation. Small settling time, small overshoot show the good dynamic characteristics and closed loop regulation of Buck converter.

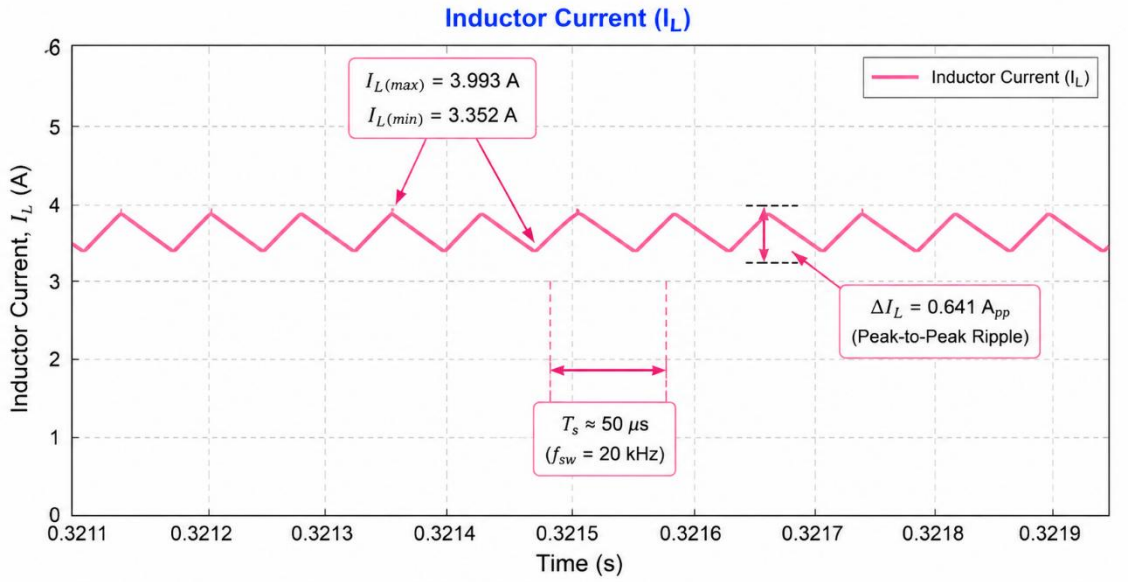

Figure 3.5 Inductor Current Waveform of Buck Converter

The inductor current ripple is calculated using:

$$\Delta\,\mathbf{I_L} = \mathbf{I_L(max)} - \mathbf{I_L(min)}$$

Substituting the measured values obtained from the simulation waveform:

$$\mathrm{I_L(max)} = 3.993\ \text{A}$$

$$\mathrm{I_L(min)} = 3.352\ \text{A}$$

Therefore,

$$\Delta\,\mathrm{I_L} = 3.993\text{-}3.352$$

$$\Delta\,\mathrm{I_L} = 0.641\ \text{A}$$

The average inductor current is observed to be approximately:

$$I_{L\ (avg)} = 3.672\ A$$

The inductor current waveform exhibits a continuous triangular ripple profile, confirming continuous conduction mode (CCM) operation of the Buck converter. During the ON-state of the MOSFET, the inductor stores energy and the current increases linearly, whereas during the OFF-state, the stored energy is transferred to the load through the freewheeling diode, causing the current to decrease gradually.

The obtained ripple current of 0.641 A indicates stable energy transfer and proper operation of the output filter components. The continuous nature of the current waveform confirms satisfactory closed-loop converter performance with controlled ripple content and stable steady-state operation.

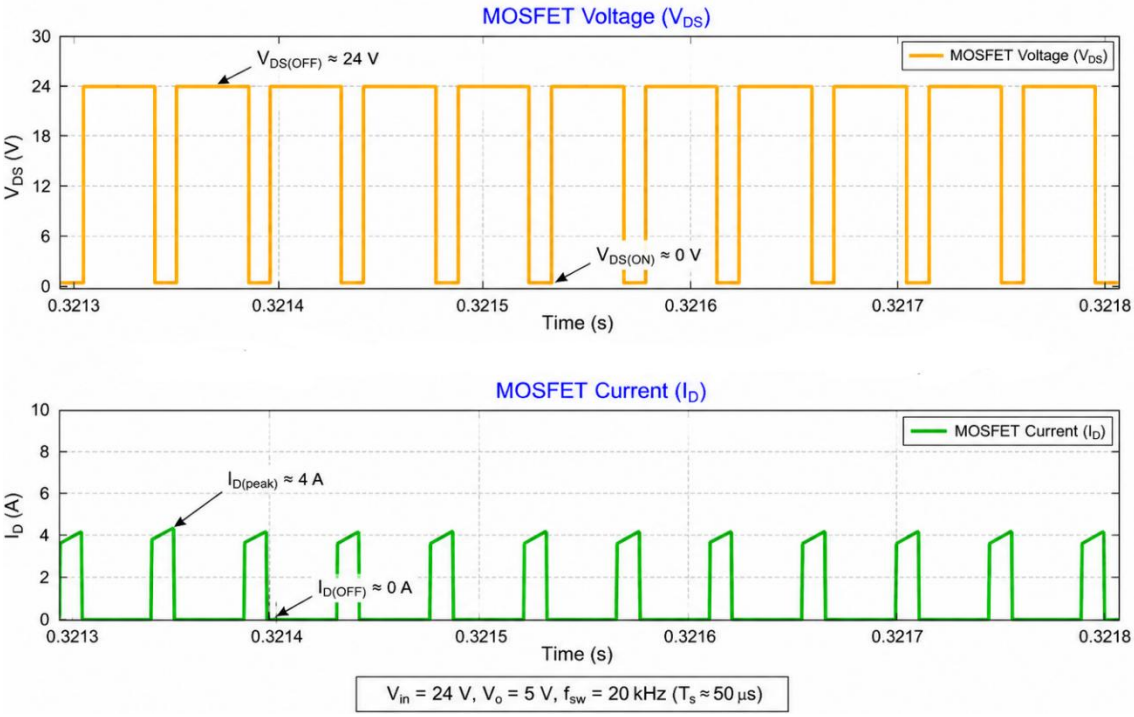

Figure 3.6 MOSFET Voltage and Current waveform

The MOSFET voltage and current waveforms confirm proper switching operation of the Buck converter under closed-loop conditions. The MOSFET voltage waveform alternates between approximately 0 V and the input voltage level of 24 V, indicating correct ON-state and OFF-state switching behaviour. During the ON-state, the voltage across the MOSFET drops nearly to zero due to conduction, whereas during the OFF-state, the MOSFET blocks the input voltage.

The MOSFET current waveform exhibits a pulsed current profile with a peak current of approximately 4 A. Current flows through the MOSFET only during the ON interval,

while during the OFF interval the current becomes nearly zero as the freewheeling diode provides the alternate conduction path for the inductor current.

The complementary nature of the voltage and current waveforms confirms effective PWM switching action and controlled energy transfer within the converter. The waveforms also indicate stable converter operation with proper switching frequency and satisfactory closed-loop performance. Overall, the obtained results validate correct MOSFET switching characteristics and reliable operation of the Buck converter under the selected operating conditions.

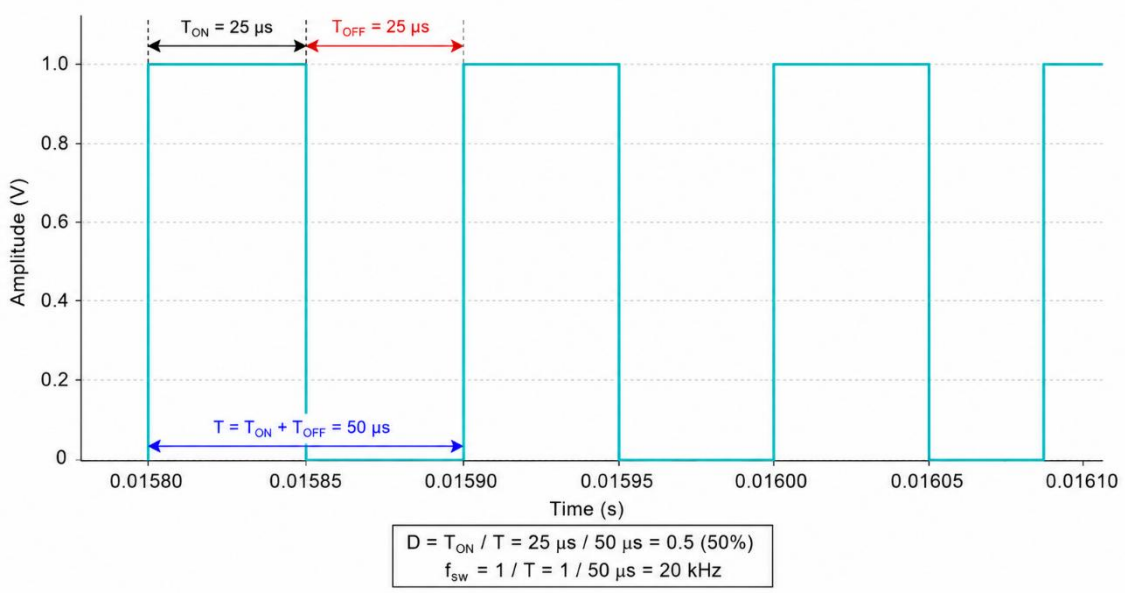

Figure 3.7 Duty Ratio Waveform

The duty ratio waveform represents the switching control action generated by the closed-loop PI controller for regulating the output voltage of the Buck converter. During transient conditions and reference variations, the duty ratio changes dynamically in order to maintain the desired output voltage. After the transient interval, the duty cycle settles to a nearly constant value corresponding to the steady-state operating condition of the converter.

The duty ratio of the Buck converter is given by:

$$D = \frac{T_{ON}}{T}$$

For the given operating condition:

$$T = 50\ \mu s$$

$$T_{ON} = 25\ \mu s$$

$$D = \frac{25}{50}$$

$$D \approx 0.5$$

The waveform confirms stable PWM switching operation and proper functioning of the closed-loop control system. The repetitive pulse pattern indicates constant switching frequency operation, while the regulated duty ratio demonstrates effective voltage control capability of the converter. The obtained results validate satisfactory dynamic response and stable steady-state performance of the closed-loop Buck converter.

Parameter	Value
Input Voltage	24 V
Initial Reference Voltage	12 V
Final Reference Voltage	5 V
Initial Duty Ratio	0.5
Final Duty Ratio	0.208
Output Voltage Ripple	≈ 5 mV
Inductor Current Ripple	0.641 A
Rated Output Power at 5 V	≈ 17.24 W
Settling Time	7–8 ms
Overshoot	7.55%

Table 3.2 Performance Parameters of Buck Converter

3.1.7 Summarizing Closed-Loop Buck Converter

A properly closed-loop regulated voltage regulation with acceptable transient response and ripple specification can be obtained using the Buck converter. The voltage converter produces acceptable low-voltage regulation levels needed for EV auxiliary applications. The study on switching characteristic, duty ratio variation and MOSFET stress is instructive on how the closed-loop converter performs.

The analysis on single Buck converter also laid the ground for the low-voltage section on integrated converter topology as explained in the sections that follow.

3.2 Negative output super lift Luo Converter

3.2.1 Introduction to NOSL Luo Converter

Negative Output Super-Lift Luo Converter (NOSL-Luo Converter), which is a DC-DC converter employing voltage-lift techniques in order to achieve negative output voltage and increase voltage transfer capacity. In comparison to the traditional boost-based

converter structures, the NOSL-Luo Converter is featured with increasing voltage gain, less voltage ripple and higher power transfer capacity.

The converter belongs to the family of Luo converters, which utilize capacitor charging and discharging principles along with voltage-lift techniques to increase output voltage in a progressive manner. Due to its ability to generate high-magnitude negative output voltage from a low DC input source, the converter is suitable for applications requiring regulated negative voltage supply.

In electric vehicle auxiliary systems, negative voltage supplies are required for communication interfaces, gate driver circuits, industrial control modules, signal conditioning systems, and certain electronic control applications. Therefore, the NOSL-Luo converter becomes suitable for generating regulated negative voltage output from a single DC input source.

In the present work, the Negative Output Super-Lift Luo Converter is analysed individually before studying the integrated converter configuration. The objective of this analysis is to study converter switching operation, voltage gain characteristics, ripple performance, transient behaviour, and closed-loop control performance under varying operating conditions.

The individual analysis of the NOSL-Luo converter also helps in understanding the high-gain negative voltage generation section later used in the integrated converter topology.

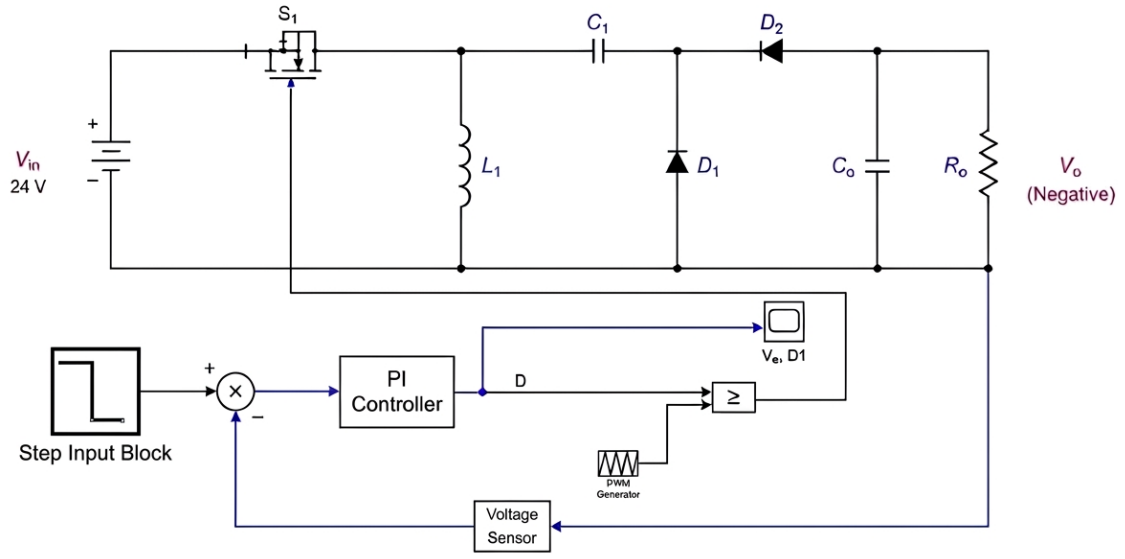

Figure 3.8 Closed-Loop Negative Output Super-Lift Luo Converter Circuit

Figure 3.9 illustrates the closed-loop Negative Output Super-Lift Luo converter used for obtaining a regulated negative DC output voltage from a positive DC input source. The converter consists of a MOSFET switch, inductor, voltage-lift capacitor, output capacitor,

diode network, PWM generator, and PI controller arranged in a closed-loop configuration for stable voltage regulation.

The MOSFET S_1 acts as the primary high-frequency switching device controlled through PWM pulses generated by the control circuit. The inductors and capacitors perform energy storage, filtering, and voltage-lift operations, while the diode network controls the charging and discharging paths of the capacitors during different switching intervals. The output capacitor C_o reduces output voltage ripple and maintains a smooth DC output across the load resistor R_o .

The closed-loop control structure continuously senses the output voltage using the voltage sensor block and compares it with the reference signal through the summing junction. The inductor L1 is the principal energy storing element for the converter. The PWM generator will compares the controller output with high-frequency carrier waveform to generate gate pulse of MOSFET switch.

The inductor L1 is the main energy storing element for the converter. The energy supplied by the input source will be stored in the inductor in the magnetic field during the ON period and it is charged up the capacitor charging path formed by diode network. When the switch is turned OFF, the stored energy of the inductor will be transferred to the output through the capacitor-diode network and negative output voltage is generated.

The characteristic of a Super-Lift Luo converter, is thevoltage-liftcapacitor C 1 C 1 which can boost up the voltage transfer capability of the converter. The capacitor C 1 is charging energy during its charging period using input and inductor network, while in discharging period the energy in the capacitor can be added in series with the inductor via the diode network so that it provides a higher negative voltage gain to output without very high duty ratio.

The voltage gain for the Negative Output Super-Lift Luo converter working in CCM can be formulated as.

$$\frac{\mathbf{Vo}}{\mathbf{Vin}} = -\frac{\mathbf{D}}{\mathbf{1-D}}$$

where:

$$\mathrm{Vo} = \text{Output voltage}$$

$$\mathrm{Vin} = \text{Input voltage}$$

$$\mathrm{D} = \text{Duty ratio}$$

The negative sign represents the phase reversal between input and output. The gain equation clearly depicts that output voltage is a rising function of duty ratio as it exploits voltage-lift nature of the converter.

The behaviour of inductor storing energy is expressed as:

$$V_L = L\frac{diL}{dT}$$

The capacitor current-voltage relationship is given by:

$$I_C = C\frac{dVC}{dT}$$

These relations describe the dynamic energy transfer process occurring within the converter during switching operation.

Overall, the closed-loop Negative Output Super-Lift Luo converter provides improved voltage boosting capability, stable negative voltage regulation, reduced ripple characteristics, and satisfactory transient response. The converter structure is suitable for low-voltage auxiliary electric vehicle applications requiring regulated negative DC output with improved voltage conversion performance.

3.2.2 Operating Principle of NOSL-Luo Converter

The Negative Output Super-Lift Luo Converter operates mainly in two switching intervals depending on the switching state of the MOSFET.

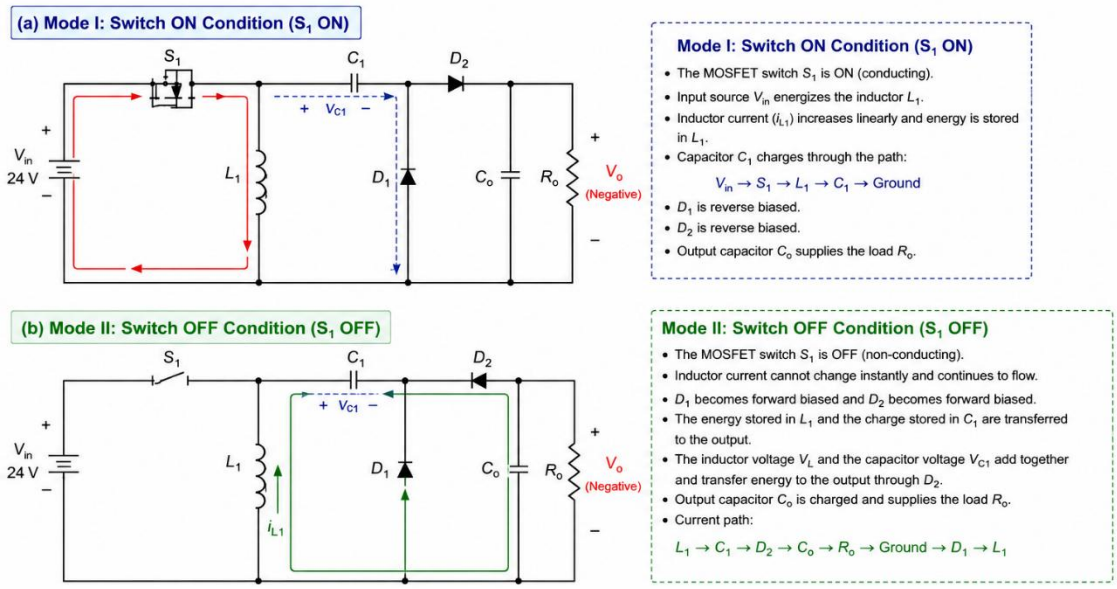

Figure 3.9 Switching Operation of NOSL-Luo Converter

I. Mode I: Switch ON Condition

During Mode I, the MOSFET switch S_1 is turned ON and the input source energizes the inductor L_1. The inductor stores energy in the form of magnetic flux, causing the inductor current to increase linearly according to:

$$V_L = L\frac{d_{il}}{dT}$$

Simultaneously, the voltage-lift capacitor C_1 charges through the switching path formed by the source, MOSFET, and inductor network. During this interval, the output capacitor C_O supplies power to the load while the diode network remains appropriately biased according to the switching condition.

II. Mode II: Switch OFF Condition

15

During Mode II, the MOSFET switch S_1 is turned OFF and the stored energy in the inductor and capacitor network is transferred to the output through the diode path. Since the inductor current cannot change instantaneously, energy continues to flow toward the load through diodes D_1 and D_2.

During this interval, the inductor voltage and capacitor voltage combine together, producing an increased magnitude of negative output voltage. The voltage conversion ratio in continuous conduction mode is given by:

$$\frac{Vo}{Vin} = -\frac{D}{1-D}$$

With negative sign indicating phase inversion at the output.

III. Voltage-Lift Operation

By the combination of C_1 and L_1, the voltage lift operation formed by C_1 and L_1 greatly increases the voltage transfer gain. While C 1 is charging, it stores the energy and in discharging period, C_1 and inductor L_1 share voltage add up through diodes, resulting increase in the negative output voltage.

The voltage lift operation described can effectively increase voltage transfer gain and enlarge the magnitude of the negative output voltage when compared to traditional converter structure.

3.2.3 Closed-Loop Control of NOSL-Luo Converter

Feedback control loop design is utilized in order to have a fixed and stable negative output voltage at various operating conditions. With the absence of feedback control loop, the output voltage may vary with load and input voltage variation.

In the present work, a PI controller is employed for regulating the output voltage. The output voltage is continuously sensed and compared with the reference signal. The error signal generated is processed through the PI controller for PWM duty ratio adjustment. The error signal is given by:

$$\mathbf{e(t) = V_{ref} - V_o(t)}$$

The controller continuously modifies the switching duty ratio to maintain stable converter operation and improve transient response characteristics.

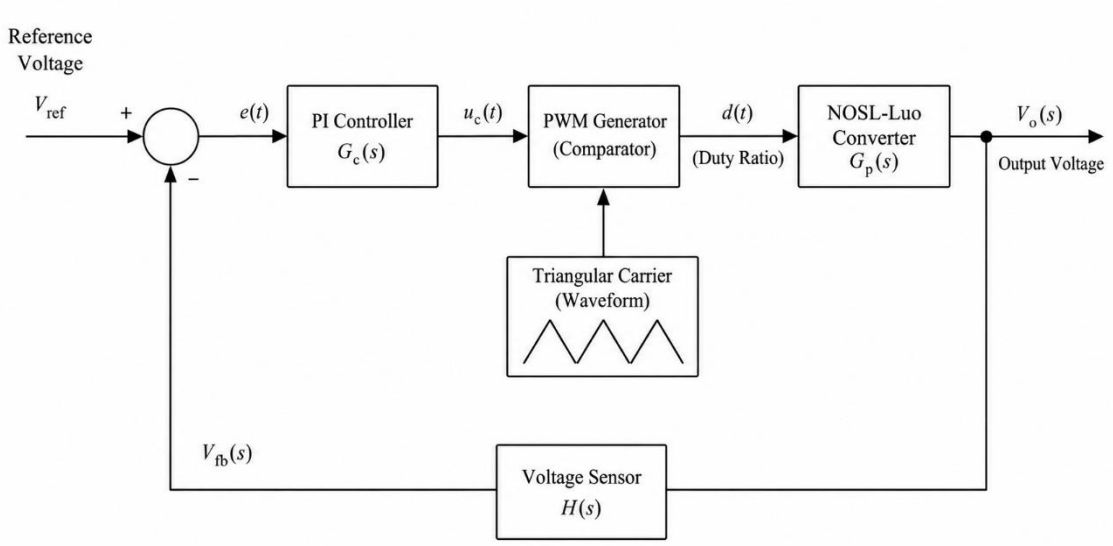

Figure 3.10 Closed-Loop Control of NOSL-Luo Converter

3.2.4 Simulation Parameters of NOSL-Luo Converter

The individual NOSL Luo converter model is implemented in MATLAB/Simulink using the same circuit parameters adopted in the integrated converter topology to evaluate its standalone closed-loop operating characteristics.

Parameter	Value
Input Voltage	24 V
Output Voltage	−48 V
Inductance	360 µH

Voltage lift capacitor	347 µF
Output capacitor	870 µF
Load Resistance	23 Ω
Switching Frequency	20 kHz
Controller	PI Controller

Table 3.3 Simulation Parameters of NOSL-Luo Converter

3.2.5 Performance Analysis of NOSL-Luo Converter

The dynamic and steady-state performance of the NOSL-Luo converter is examined through the analysis of output voltage regulation, inductor current response, MOSFET switching characteristics, and duty cycle variation obtained from simulation results.

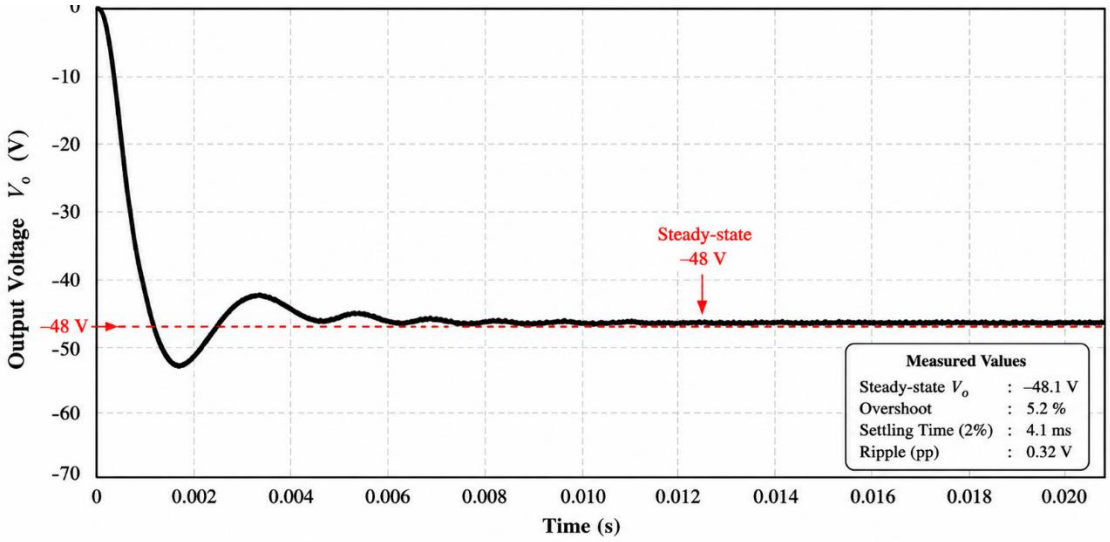

Figure 3.11 Output Voltage Waveform of NOSL-Luo Converter

The output voltage waveform confirms stable closed-loop operation of the Negative Output Super-Lift Luo converter. The converter successfully generates the required high-gain negative output voltage of approximately −48 V with satisfactory transient and steady-state performance. After the initial start-up transient, the output voltage settles to the reference value with reduced oscillations and stable voltage regulation.

This waveform is evidence that the PI controlled PWM switching technique is also successful in controlling the output voltage to the required value during operation. It shows that the converter has reasonable settling time and is not being overshot to too great an extent during operation.

The output voltage ripple is determined using:

$$\mathbf{\Delta Vo = Vo(max) - Vo(min)}$$

From the steady-state waveform:

$$\mathrm{Vo(max)} \approx -47.9\ \mathrm{V}$$

$$\mathrm{Vo(min)} \approx -48.2\ \mathrm{V}$$

Therefore,

$$\mathbf{\Delta Vo \approx 0.3\ V}$$

The small value of the output voltage ripple guarantees the filter action of the output capacitor and the smooth transfer of energy by the voltage-lift network. The output voltage waveform shows good capability of closed-loop voltage regulation and the dynamic response of NOSL-Luo converter.

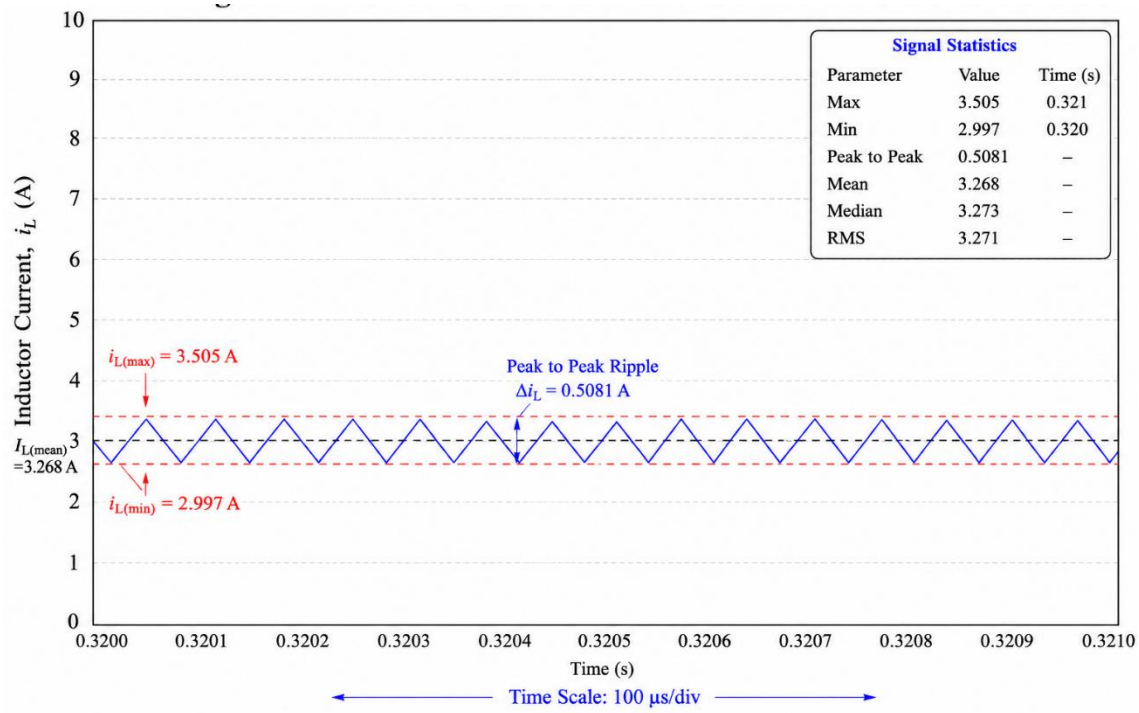

Figure 3.12 Inductor Current Waveform of NOSL-Luo Converter

The inductor current waveform illustrates the stable CCM operation of NOSL-Luo converter. It can be seen that the current of the inductor has a smooth and continuous triangular waveform because the high frequency PWM switching effect ensures the complete conduction and energy transfer through the inductor for the whole switching period.

The inductor current ripple is calculated using:

$$\mathbf{\Delta I_L = \Delta I_{Lmax} - \Delta I_{Lmin}}$$

From the waveform statistics:

$$\mathrm{I_{Lmax}} = 3.505\ \mathrm{A}$$

$$I_{Lmin} = 2.997\ A$$

Therefore,

$$\Delta I_L = 3.505 - 2.997$$

$$\mathbf{\Delta I_L = \approx 0.508\ A}$$

The average inductor current is observed as:

$$I_{Lmean} \approx 3.268\ A$$

The relatively low ripple current confirms proper inductor selection and stable converter operation under closed-loop conditions. The waveform also verifies periodic charging and discharging operation of the converter energy storage elements responsible for voltage-lift action and output power transfer.

The MOSFET voltage waveform confirms proper switching operation of the converter. During the ON-state, the MOSFET conducts and the voltage across the switch approaches zero due to low ON-state resistance. During the OFF-state, the MOSFET blocks the applied converter voltage and experiences the corresponding switch voltage stress.

The observed switching waveforms validate correct PWM operation, stable energy transfer, and satisfactory dynamic performance of the NOSL-Luo converter under closed-loop control operation.

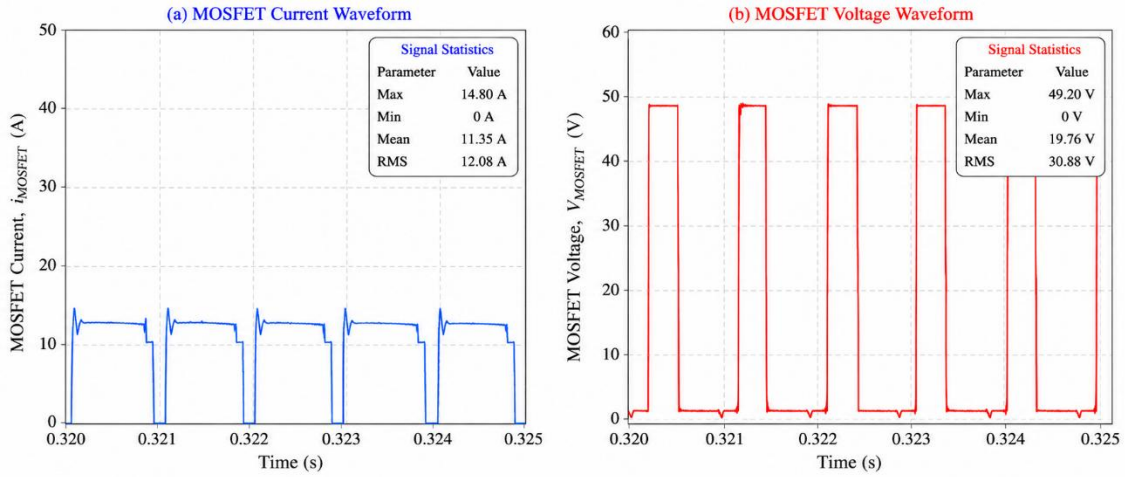

Figure 3.13 MOSFET current and MOSFET voltage waveform

under closed-loop conditions. The waveforms exhibit periodic switching characteristics corresponding to the PWM-controlled operation of the converter.

The MOSFET current waveform shows pulsed current behaviour during the conduction interval of the switch. When the MOSFET is turned ON, the switch carries the inductor current and energy is transferred from the source to the converter energy storage elements. The observed current ripple is associated with the charging and discharging action of the

inductor and voltage-lift capacitor network. Short-duration current spikes are visible during switching transitions due to capacitor charging current and high-frequency switching effects.

The MOSFET voltage waveform exhibits complementary behaviour with respect to the current waveform. During the ON-state, the voltage across the MOSFET approaches zero because of switch conduction. During the OFF-state, the MOSFET blocks the converter voltage and experiences the corresponding voltage stress. The observed switching transitions confirm effective PWM gating and stable switching operation.

The waveforms validate stable converter operation in continuous conduction mode and confirm satisfactory dynamic performance of the closed-loop NOSL-Luo converter. The switching behaviour also verifies proper operation of the voltage-lift energy transfer mechanism responsible for generating the regulated negative output voltage.

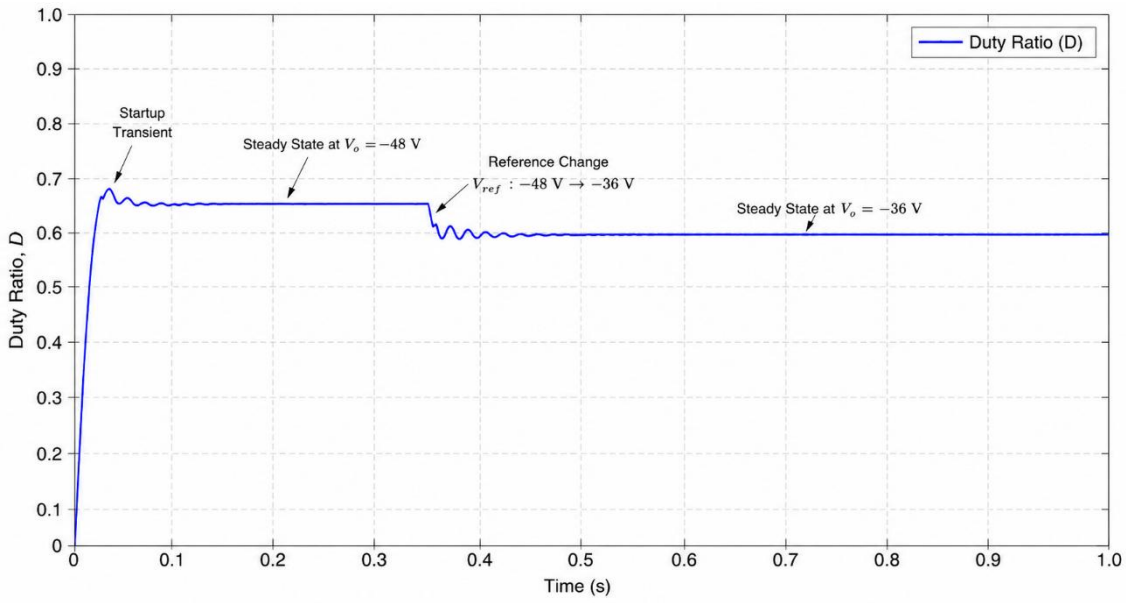

Figure 3.14 Duty Ratio Waveform

The duty ratio waveform demonstrates the dynamic PWM control action of the closed-loop Negative Output Super-Lift Luo converter. During startup and transient operating conditions, the PI controller continuously adjusts the duty ratio according to the error between the reference voltage and sensed output voltage in order to maintain stable voltage regulation.

Initially, a higher duty ratio is observed because of the large startup error. After a short transient interval, the waveform settles to a steady-state operating value corresponding to the required output voltage. When the reference voltage is changed from (-48,V) to (-

36,V), the controller modifies the duty ratio and the waveform reaches a new steady-state condition after a damped transient response.

The duty ratio relation for the NOSL-Luo converter operating in continuous conduction mode is given by:

$$D = \frac{V_O}{V_O + V_{in}}$$

For an input voltage of 24V and output voltage of -48V the theoretical duty ratio is calculated as:

$$D = \frac{48}{48+24} = 0.667$$

Similarly, for an output voltage of -36V, the theoretical duty ratio becomes:

$$D = \frac{36}{36+24} = 0.6$$

The obtained waveform closely follows the theoretical operating duty ratio values and validates proper closed-loop control performance of the converter.

Parameter	Value
Input Voltage	24 V
Output Voltage	−36 V to −48 V
Voltage Gain	$-\frac{D}{1-D}$
Output Voltage Ripple	0.3 V
Inductor Current Ripple	0.508 A
Rated Output Power	100.8 W
Output Current	2.1 A
Settling Time	10 ms
Overshoot	13.20%
Duty Ratio Range	0.60–0.67
Voltage Conversion Ratio	1.5–2.0
Switching Stress	Comparatively High
Number of Active Switches	1
Number of Inductors	1
Number of Capacitors	2
Output Polarity	Negative

Table 3.4 Performance Parameters of NOSL-Luo Converter

The Negative Output Super-Lift Luo converter demonstrates stable high-gain negative voltage generation under closed-loop operating conditions. The converter successfully regulates the negative output voltage with acceptable ripple content, satisfactory transient response, and continuous energy transfer operation.

The analysis of converter switching modes, voltage-lift operation, ripple characteristics, and dynamic response confirms effective operation of the converter under varying reference voltage conditions. The PI-controlled closed-loop structure provides stable output voltage regulation by continuously adjusting the PWM duty ratio according to the system error.

The obtained results verify the capability of the NOSL-Luo converter to achieve high voltage gain with controlled output ripple and stable transient performance. The individual analysis of the converter also provides the necessary understanding of the high-gain negative voltage generation stage, which forms the basis for the integrated converter topology discussed in the subsequent chapter.

3.3 Comparative Analysis of Individual Converter Topologies

Parameter	Buck Converter	NOSL-Luo Converter
Input Voltage	24 V	24 V
Output Voltage	12 V → 5 V	−48 V → −36 V
Voltage Gain	0.50 → 0.21	2.0 → 1.5
Output Voltage Ripple	6.35 mV	0.3 V
Inductor Current Ripple	0.641 A	0.508 A
Output Current	8.28 A → 3.45 A	2.09 A → 1.57 A
Output Power	99.31 W → 17.24 W	100.17 W → 56.35 W
Settling Time	7–8 ms	10.8 ms
Overshoot	7.55%	13.20%
Duty Ratio Range	0.50 → 0.21	0.67 → 0.60
Voltage Conversion Ratio	0.50 → 0.21	2.0 → 1.5
Switching Stress	Low	Comparatively High
Number of Active Switches	1	1
Number of Inductors	1	1
Number of Capacitors	1	2
Output Polarity	Positive	Negative

Table 3.5 Comparative Performance Analysis of Individual Converter Topologies

The individual analysis of the Buck converter and Negative Output Super-Lift Luo (NOSL-Luo) converter provides a clear understanding of their operating characteristics, voltage conversion capability, dynamic response, and switching performance under closed-loop operating conditions.

The Buck converter operates as a low-voltage step-down converter and produces regulated positive output voltage suitable for low-power auxiliary electronic loads. Due to its simple topology and reduced conversion ratio, the converter exhibits low output

voltage ripple, comparatively lower switching stress, and fast transient response. The closed-loop PI controller maintains stable voltage regulation during startup and reference variation conditions with satisfactory settling time and controlled overshoot characteristics.

In contrast, the NOSL-Luo converter operates as a high-gain negative output converter capable of generating larger magnitude negative voltage from the same input source. Voltage-lift capacitor network, it is found to greatly boost the voltage conversion gain, as well as providing a regulated negative polarity output. Hence it is advantageous for communication circuits, gate drive circuits and other negative auxiliary supplies. However the converter is suffering relatively high switching stresses and transient overshoot compared to the Buck converter due to its high-gain operation and capacitor-assisted energy transfer.

With respect to ripple analysis, the Buck converter is found to produce low-voltage with small ripple by using conventional LC filter. The NOSL-Luo converter has higher voltage gain with satisfactory ripple characteristic under conduction mode.

In terms of transient analysis, both converters are found to exhibit stable closed-loop response under step changes of the reference voltage. The PI controller always adjusts the PWM duty ratio according to the system error, and provides regulated voltage output during start up as well as under transient disturbance. Settling time of the Buck converter is generally quicker compared to NOSL-Luo converter. Because the voltage-lift capacitor network has more complex charging and discharging process,NOSL-Luo has relatively longer settling time.

For the switching waveform analysis, it is found that switching stresses of the MOSFET in NOSL-Luo converter are significantly higher than that of the Buck converter due to its high voltage gain, energy transfer amount and power devices utilization. By contrast, it is seen that switching stress in the Buck converter is more suitable.

Individual converter analysis demonstrates that Buck converter is a proper choice for a low-voltage regulated auxiliary supply. NOSL-Luo converter is proper for high-gain negative voltage supply. Through the analysis of both individual circuits, it builds up a foundation for analysis of the integrated converter.

3.4 Need for Integrated Converter Structure

It is clear that individual Buck and Negative Output Super-Lift Luo (NOSL-Luo) converter perform reasonably good for respective required voltage conversion ratio in

closed loop. Buck converter is the right choice for the regulated low-voltage positive output, where the NOSL-Luo converter is appropriate for regulated high-gain negative output voltage generation.

Nevertheless, for practical EV auxiliary power supply system, more than one regulated output voltages are required simultaneously from a single DC input. Using different individual converter topology to generate both positive and negative voltage outputs increase overall components number, converter size, gate driving hardware, switching losses, and the system control complication. More over, for individual operation of converter, higher required hardware and lower degree of power conversion density.

Buck converter has the benefit of low-voltage step-down with low output voltage ripple and lower switching loss where NOSL-Luo has benefit of higher voltage gain and negative voltage with voltage lift stage. Although both topologies perform good in individual working, it does not fulfill the requirements of compact multi-output application.

Thus, an effective solution is to integrate Buck converter with NOSL-Luo converter to generate simultaneous regulated positive and negative output voltage from a single input with the common active switching network. By integrating them, the complexity of hardware, active switches number, converter size and utilizing rate of input source can be greatly minimized.

Combined the low-voltage step-down capability of Buck converter with the high voltage gain negative output of NOSL-Luo converter, regulated both output voltages with a single closed loop control strategy which result to the dual output converter as analyzed in following chapter.

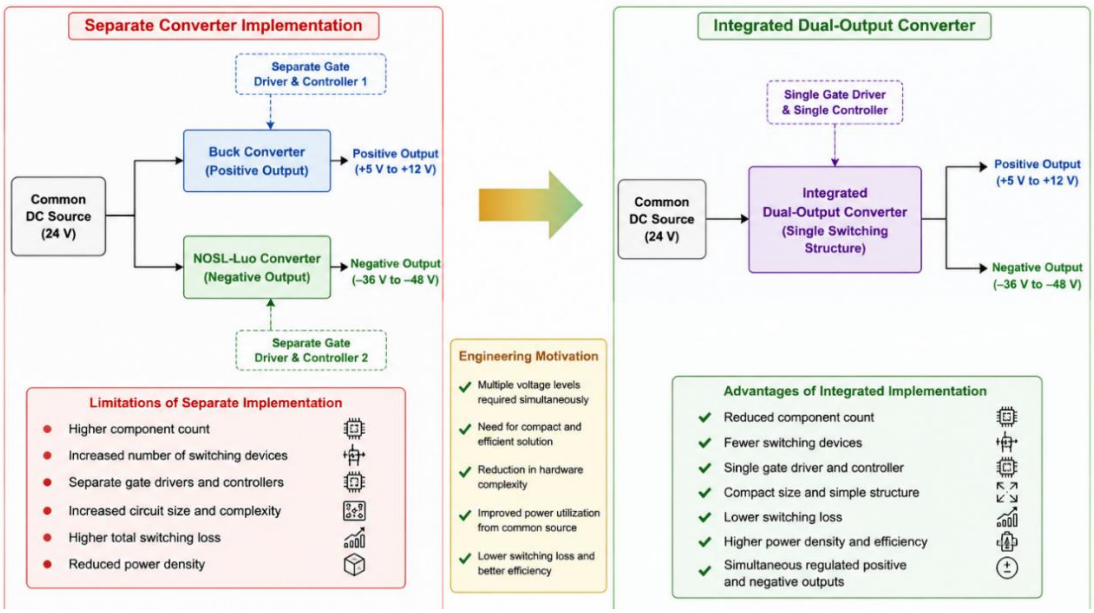

Figure 3.15 Need for Integrated Dual-Output Converter

CHAPTER 4

INTEGRATED BUCK–NOSL LUO CONVERTER-CONVERTER TOPOLOGY AND OPERATION

4.1 Introduction

This chapter introduces the integrated converter configuration which is implemented by merging Buck converter and NOSL-Luo converter to form a combined dual-output converter topology. The intended converter topology produces unregulated positive and negative outputs from a common DC voltage source using a shared switching structure.

The integrated configuration merges the low-voltage regulating feature of Buck converter and high-voltage boosting ability ofNOSL-Luo converter to produce regulated positive and negative output voltages, which can be used for control circuits, gate driver circuits, communication devices, sensors and other low power auxiliary electronic loads in automotive applications.

The proposed converter operates under closed-loop control using a PI controller and PWM switching technique to maintain stable output voltage regulation under varying operating conditions.

4.2 Integrated Converter Topology

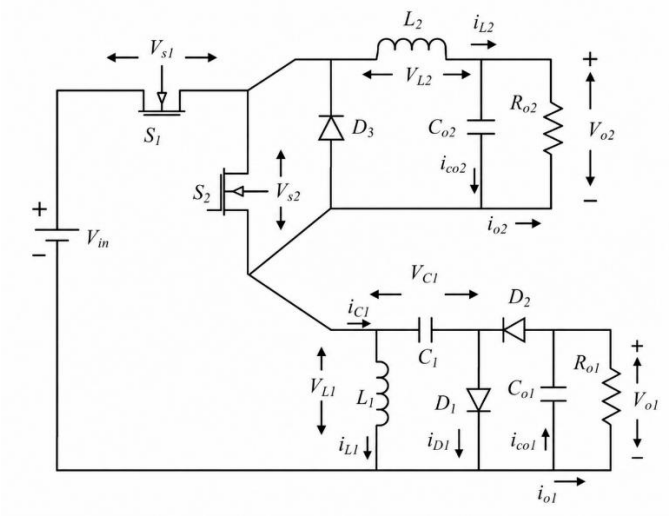

Figure 4.1 Integrated Buck–NOSL Luo converter

The Modelled integrated converter combines the Buck converter and Negative Output Super-Lift Luo (NOSL-Luo) converter into a single dual-output converter structure operating from a common DC input source. The integrated topology is developed to simultaneously generate regulated positive and negative output voltages required for auxiliary electric vehicle applications.

The converter consists of a common switching structure, inductors, capacitors, diodes, output filter sections, and closed-loop control circuitry. The Buck converter section provides regulated low-voltage positive output, whereas the NOSL-Luo section generates high-gain negative output voltage through voltage-lift operation. Both output stages are supplied from the same input source and share common converter components, thereby reducing the overall hardware complexity compared to separate standalone converter structures.

The proposed converter operates with a 24V DC input source and produces two regulated outputs:

- Positive low-voltage output through the Buck converter section
- High-gain negative output through the NOSL-Luo section

The integration of both converter sections enables simultaneous dual-output operation using a reduced number of switching devices and control components structure, thereby reducing overall component count and improving converter compactness.

The PI controller continuously senses the output voltage and adjusts the PWM duty ratio according to the system error in order to maintain stable closed-loop regulation.

4.3 Power Flow in Integrated Converter

The input power supplied by the DC source is distributed between the Buck converter section and the NOSL-Luo converter section through the common switching network. During the switching operation, energy transfer takes place through controlled charging and discharging of inductors and capacitors.

When the main switch is turned ON:

- the inductors store energy from the input source,
- the Buck converter section transfers energy to the positive output load,

- and the voltage-lift capacitor network of the NOSL-Luo section gets charged through the diode conduction path.

In the OFF interval,

- The energy stored in the inductors is dumped into the output loads.
- The charged voltage-lift capacitors are discharged through the diode network.
- The magnitude of negative output voltage increases because of the help of capacitor to transfer energy to output.

The integrated topology not only enable transferring power to both output stages simultaneously but also enables the closed-loop operation to regulate the output voltages..

I. Positive Output Section

The working of the positive output section of the integrated converter is analogous to Buck converter. The output voltage is regulated by controlling the PWM duty ratio of the switching device through the PI controller.

The Buck converter section provides:

- regulated low-voltage positive output,
- reduced output voltage ripple,
- fast transient response,
- and comparatively lower switching stress.

The output voltage relation for the Buck converter section operating in continuous conduction mode is given by:

$$\mathbf{V_{o1} = DV_{in}}$$

where:

$$V_{o1} = \text{Positive output voltage}$$

$$D = \text{Duty ratio}$$

The positive output stage is suitable for supplying low-voltage auxiliary electronic loads such as sensors, controllers, communication modules, and low-power embedded systems.

II. Negative Output Voltage Equation (NOSL-Luo Section)

The negative output section operates based on the Negative Output Super-Lift Luo converter topology. The converter generates high-gain negative voltage using voltage-lift operation achieved through controlled charging and discharging of capacitors.

The NOSL-Luo section consists of:

- inductors,

- voltage-lift capacitors,
- diode network,
- output filter capacitor,
- and load section.

The output voltage relation of the NOSL-Luo converter operating in continuous conduction mode is expressed as:

$$\mathbf{Vo} = -\frac{\mathbf{D}}{\mathbf{1-D}}\mathbf{Vin}$$

where:

Vo= Output voltage

Vin= Input voltage

D = Duty ratio

The negative polarity output is suitable for:

- gate driver circuits,
- communication interfaces,
- signal conditioning circuits,
- and auxiliary negative voltage applications.

III. Voltage-Lift Mechanism of NOSL-Luo Section

The voltage-lift mechanism is the essential step and operation principle by which high voltage conversion gain can be obtained in the Negative Output Super-Lift Luo converter stage. Unlike a traditional converter configuration using purely inductive energy transfer for energy transfer, the NOSL-Luo converter uses a voltage lifting via capacitor for increased negative output voltage magnitude.

The voltage-lift capacitor is charged and discharged alternately according to the operation switching condition of the MOSFET. In the MOSFET ON phase, the inductor energy will be stored from the input voltage source, whereas the voltage-lift capacitor charges through the diode network according to the converter circuit path. This charging process in the capacitor stores electrical energy in the form of electrostatic field energy.

During the MOSFET OFF phase, the stored inductor energy and the charged capacitor energy simultaneously supply to the output stage. This stage effectively causes the capacitor voltage to combine with the input source voltage via the diode network. This

step of summing voltages drastically increases the negative output voltage magnitude as opposed to typical converter topologies.

The operation of combining voltages is what allows the converter to attain an improved voltage gain without necessarily operating with a greatly large duty ratio. The combined contribution of:

- source voltage,
- inductor energy,
- and capacitor stored energy

results in higher voltage transfer capability during the OFF interval.

The output voltage relation of the NOSL-Luo converter is given by:

$$\mathbf{Vo} = -\frac{\mathbf{D}}{\mathbf{1-D}}\mathbf{Vin}$$

where:

Vo= Output voltage

V_{in}= Input voltage

D = Duty ratio

As the duty ratio increases, the voltage-lift operation enhances the output voltage magnitude significantly.

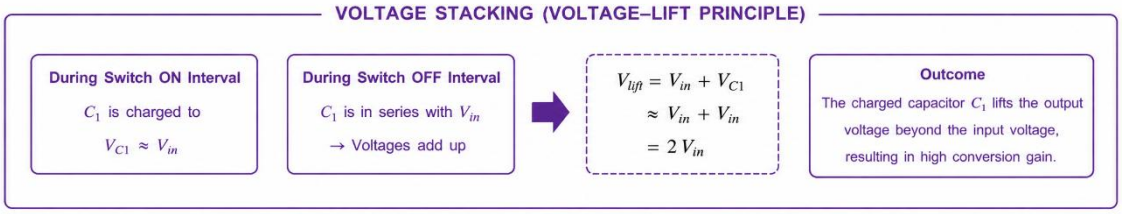

Figure 4.2 Voltage-Lift Energy Transfer Mechanism

With reference to traditional Boost converter, the NOSL-Luo converter possess superior voltage gain capability resulting from its capacitor-aided energy transfer.

A conventional Boost converter primarily depends on inductive energy transfer for voltage boosting, whereas the NOSL-Luo converter combines inductive energy transfer with voltage-lift capacitor action to achieve higher gain.

The conventional Boost converter voltage gain relation is:

$$\mathbf{V_{o1}} = \mathbf{DV_{in}}$$

Although both converters provide voltage boosting capability, the NOSL-Luo converter achieves:

- higher voltage gain,

- negative polarity output,
- improved gain enhancement,
- and better suitability for high-gain auxiliary applications.

The voltage-lift capacitor network therefore performs multiple important functions within the converter operation:

- capacitor-assisted energy transfer,
- voltage stacking,
- gain enhancement,
- transient energy support,
- and high-gain negative voltage generation.

This voltage-lift mechanism forms the key advantage of the NOSL-Luo section within the proposed integrated converter topology.

4.4 Operating Modes of integrated Converter

The proposed Negative Output Super-Lift Luo (NOSL-Luo) converter operates in Continuous Conduction Mode (CCM) and consists of four operating modes within one switching cycle. The switching operation of MOSFETs S_1 and S_2 along with the charging and discharging behaviour of inductors and capacitors, determines the voltage transfer characteristics of the converter.

I. Mode I Operation (0<t<t1)

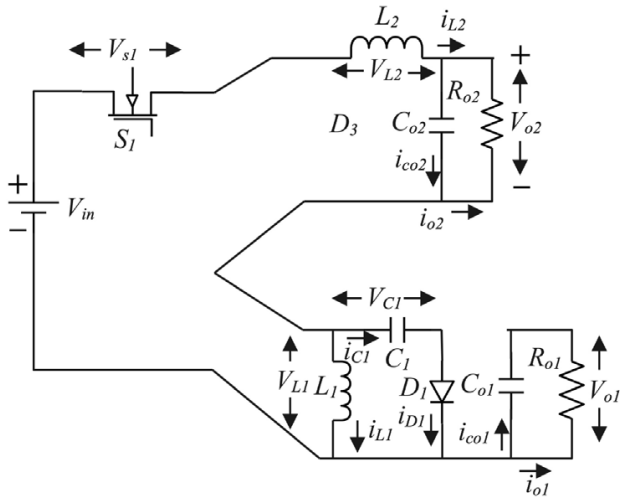

Figure 4.3 Mode 1 operation

During Mode I operation, switch S_1 is turned ON while switch S_2 remains OFF. Under this condition, the input source energizes inductor L_1, and the energy previously stored in L_1 is transferred to inductor L_2 and the output side.

Diode D_1 becomes forward biased, whereas diodes D_2 and D_3 remain reverse biased. The capacitor C_1 starts charging through the converter current path. Simultaneously, output capacitor C_{o2} supports the load current during transient energy transfer.

The current path is established from:

$$\mathbf{V_{in} \rightarrow S_1 \rightarrow L_1 \rightarrow L_2 \rightarrow R_{o2}}$$

During this interval:

- L_1 stores energy from the source,
- L_2 receives transferred energy,
- C_1 charges,
- C_{o2} filters output ripple.

Applying Kirchhoff's Voltage Law (KVL):

$$\mathbf{Vin = V_{o2} + V_{L1} + V_{L2}}$$

The inductor currents increase gradually due to the positive applied voltage across the inductors.

Applying Kirchhoff's Current Law (KCL):

$$\mathbf{i_{in} = i_{L1} + i_{C1}}$$

This mode mainly contributes to:

- initial energy storage,
- capacitor charging,
- and preparation for voltage-lift operation in subsequent modes.

II. Mode II Operation (t1<t<t2)

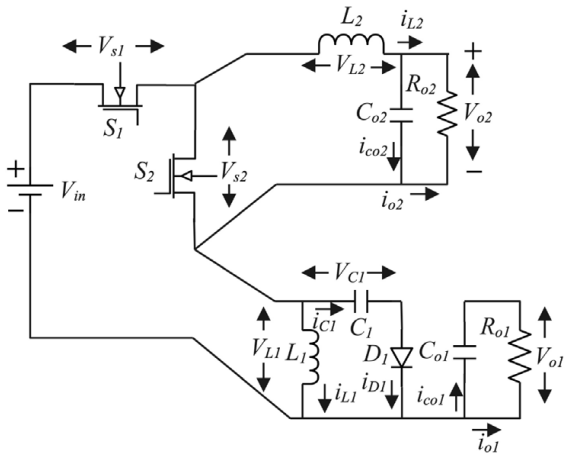

Figure 4.4 Mode 2 operation

In Mode II, both switches S_1 and S_2 are turned ON simultaneously. The source directly energizes inductor L_1, while the energy stored in inductor L_2 is discharged to the load through the output section.

Diodes D_2 and D_3 remain reverse biased during this interval. Capacitor C_1 continues storing charge energy required for the voltage-lift mechanism.

The current path for the output side is:

$$\mathbf{L_2 \rightarrow C_{o2} \rightarrow R_{o2}}$$

During this interval:

- L_1 is charged by the source,
- L_2 releases stored energy,
- C_{o2} supports output regulation.

Applying KVL across the output loop:

$$\mathbf{V_{o2} = -V_{L2}}$$

Applying KCL:

$$\mathbf{i_{L2} = i_{Co2} + i_{o2}}$$

This mode is responsible for:

- maintaining load current continuity,
- reducing output ripple,
- and sustaining CCM operation.

III. Mode III Operation (t2<t<t3)

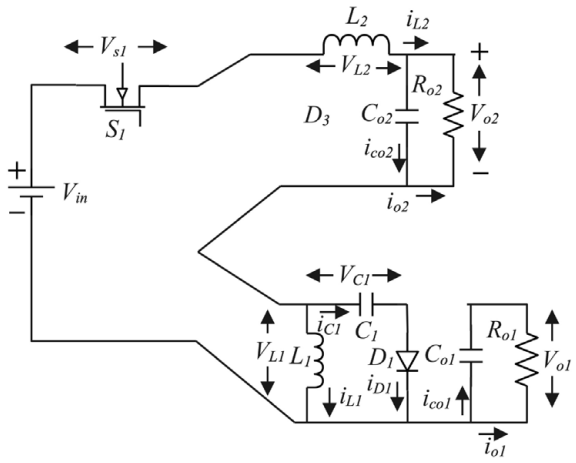

Figure 4.5 Mode 3 operation (Similar to mode 1)

Mode III operation is identical to Mode I. Switch S_1 remains ON while switch S_2 remains OFF. The converter again transfers energy from the source and inductors toward the output stage.

The capacitor C_1 continues participating in the voltage-lift charging process. Inductor L_1 stores energy while L_2 supports the output load.

The same current paths and governing equations of Mode I are applicable in this interval.

This repeated operating interval ensures:

- continuous energy transfer,
- improved voltage boosting,
- and stable converter operation under closed-loop conditions.

IV. Mode IV Operation (t3<t<t4)

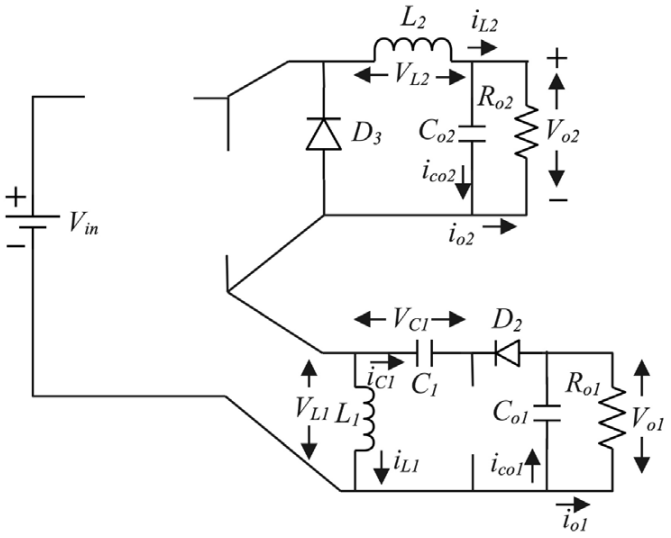

Figure 4.6 Mode 4 operation

During Mode IV, both switches S_1 and S_2 are turned OFF. This is the most important operating interval responsible for voltage-lift action and high voltage gain generation.

The stored energy in inductors L_1 and L_2, along with the charged capacitor C_1, is transferred to the output load through diodes D_2 and D_3.

In this mode:

- diode D_1 becomes reverse biased,
- diodes D_2 and D_3 become forward biased,
- capacitor C_1 discharges,
- voltage stacking operation occurs.

The current path is established through:

$$\mathbf{L_1 \rightarrow C_1 \rightarrow D_2 \rightarrow R_{o1}}$$

and

$$\mathbf{L_2 \rightarrow D_3 \rightarrow R_{o2}}$$

During this interval:

- ❖ inductors release stored magnetic energy,
- ❖ capacitor C_1 releases electrostatic energy,
- ❖ output capacitors maintain voltage regulation.

Using KVL for NOSL output section:

$$\mathbf{V_{o1} = V_{C1} - V_{L1}}$$

The fact that capacitor C1 was charged up during the previous modes.

$$V_{C1}=V_{in}$$

Applying KCL:

$$i_{L1}=-i_{C1}=i_{Co1}+i_{o1}$$

This interval of operation can yield:

- ❖ voltage-lift action;
- ❖ voltage stacking;
- ❖ increased negative output voltage;
- ❖ high conversion gain.

The combined effort from the source voltage, capacitor voltage, and energy stored in the inductor, cumulatively contributes to producing a negative output voltage that is orders of magnitude greater in magnitude than the output of traditional converter topologies.

V. Technical Discussion of Overall Mode Operation

The four modes of operation as mentioned above contribute to constant energy flow between source, storing elements and output load. This charging/discharging of inductors and capacitors form the underlying principle of the voltage-lift mechanism in NOSL-Luo converter. The converter realizes

1. High voltage transfer gain.
2.regulated negative output voltage
3. Low output ripple
4. Continuous conduction mode operation
5. Stable closed loop behavior.

All this, with an efficient interplay of inductors L_1 and L_2, voltage-lift capacitor C_1, output capacitors and diode network for conversion, boosts voltage in comparison to existing boost converter structure.

4.5 Voltage gain derivation

Under ideal working conditions, where semiconductors are loss less and passive elements are ideal, and the ripple in the inductor currents and in capacitor voltages is zero, we derive the voltage transfer gain (VTG) of the Integrated Converter. The voltage transfer characteristics of the converter are calculated from the volt-second balance on the inductors in steady state conditions.

The given converter is the integration of the Negative Output Super-Lift Luo Converter with a buck stage converter. The voltage transfer gain in case of NOSL Luo converter

mainly relies on d2. While the step down converter has its gain depending on d1 and d2 both. Applying volt-second balance to the inductor during one switching period:

$$\mathbf{V_{in} d_2 T_S = [(V_{o1} - V_{in})(1 - d_2)]T_S}$$

Rearranging the above equation:

$$\mathbf{[V_{in} = V_{o1}(1 - d_2)]T_S}$$

Therefore, the voltage transfer gain of the NOSL Luo Converter is obtained as:

$$\mathbf{G_1 = \frac{V_{o1}}{V_{in}} = (\frac{2 - d_2}{1 - d_2} - 1)}$$

Similarly, the voltage transfer gain of the buck converter output is derived as:

$$\mathbf{d_2 V_{o2} = \left[d_2 - d_1 + d_1 - d_2 \left(\frac{1}{1-d_2}\right)\right] V_{in}}$$

Further simplification gives:

$$\mathbf{G_2 = \frac{V_{o2}}{V_{in}} = \left(\frac{d_2 - 1}{1 - d_2} + 1\right)}$$

The derived equation for the voltage transfer gain showed that the NOSL Luo Converter output voltage is greatly dependent on duty cycle $d2$, while the step-down output voltage is dependent on the synergistic effects of $d1$ and d_2. This characteristic of the circuit enables versatility in voltage regulation and a single converter unit can produce different levels of output voltages. The circuit is quite suitable for EV applications, as varying subsystems in the EV require varying voltage levels. The described converter can deliver both stepped up as well as stepped down regulated output voltages with adequate voltage conversion ratio if $d1$ and $d2$ are controlled in appropriate manners.

4.6 Design Specifications

This designed single integrated dual output converter is capable of providing the regulated positive and negative voltages from a common dc source. It's intended for low-voltage auxiliary applications and high-gain negative output voltage applications. Design parameters are specified such that it will result in stable closed-loop operation, controllable ripple, and efficient power delivery under all specified load condition and input variation.

This converter uses regulated 24 V DC input source. The Buck converter can be found that provides a regulated positive output voltage (12-5 V) via a reference voltage control, and the Negative Output Super-Lift Luo (NOSL-Luo) converter can be found that produces a regulated negative output voltage (-48 to -36 V).

The PWM operation uses a switching frequency of 20 kHz so that steady switching operation can be obtained and dynamic response is adequate and excessive switching loss will not cause problem. Continuous Conduction Mode (CCM) operation is assumed such that current flow in inductors will be continuous during a switching cycle.

Under the rated load condition, the converter outputs will have a near to 100W power. Under a reference voltage variation, the output voltage changes, so does the power under the corresponding load.

The output voltage ripple and inductor current ripple are maintained within acceptable limits to reduce stress on switching devices and improve output regulation performance. The Buck converter exhibits lower ripple characteristics due to step-down operation, while the NOSL-Luo converter achieves higher voltage gain with acceptable ripple under closed-loop control.

The design specifications considered for the converter are:

- Input Voltage, Vin = 24 V
- Output Voltage, V_O = 48 V
- Output Power, P_O= 100 W
- Switching Frequency, F_S= 20 kHz

The duty ratios of the proposed converter are determined using the voltage gain relations of the integrated converter topology.

The duty ratio d1 is calculated as:

$$\mathbf{D_2} = \frac{V_{01}}{V_{IN}} = \frac{1}{1-D_2} = \mathbf{0.5}$$

$$\mathbf{D_1} = \frac{D_1-1}{1-D_2} + 1 = \mathbf{0.75}$$

The calculation of inductance is performed by the following relation:

$$L1 = \frac{Vin * D_2}{F_S * \Delta I_{L1}}$$

L1= 720 µH

$$L2 = \frac{Vin * (1 - D_2)}{F * \Delta I_L}$$

L2= 360 µH

The calculation of ripple current of boost inductance is performed by the following relation:

$$\Delta I_L = 0.2 * \frac{Vo}{V_{in}} * I_o$$

ΔI_{L2} = 16.67A

ΔI_{L1} = 0.416A

The coupling capacitance value of Luo converter is provided by the following relation:

$$\mathbf{C_s = \frac{I_L * D}{\Delta V_c * F_s}}$$

Cs = 347 µF

The capacitance value at the load side is provided by the following relation:

$$\mathbf{C_{out} \geq \frac{I_{out} * D}{V_{ripple} * 0.5 * f_{sw}}}$$

Cout 1 = 540 µF

Cout 2 = 870 µF

The ripple output voltage is calculated as 2% of the output voltage and is given by

$$\Delta V_{oc} = 0.02 V_o$$

$$\mathbf{\Delta V_{oc} = 0.96V}$$

Parameter	Symbol	Value
Input Voltage	V_{in}	24 V
Positive Output Voltage (Buck)	V_{o2}	+12 V
Negative Output Voltage (NOSL-Luo)	V_{o1}	−48 V
Buck Duty Ratio	D_1	0.5
NOSL-Luo Duty Ratio	D_2	0.67
Switching Frequency	f_s	20 kHz
Buck Inductor	L_2	360 µH
Luo Inductor	L_1	720 µH
Buck Output Capacitor	C_{o2}	540 µF
Luo Output Capacitor	C_{o1}	870 µF
Luo Lift Capacitor	C_1	347 µF
Buck Load Resistance	R_{o2}	1.45 Ω
Luo Load Resistance	R_{o1}	23 Ω
PI Controller Proportional Gain	Kp	0.46
PI Controller Integral Gain	Ki	0.002
Control Method	—	Closed-Loop PI Control
Mode of Operation	—	CCM

Table 4.1 Design Specifications of Integrated Buck–NOSL Luo Converter

4.8 Closed-Loop Control Structure

The proposed integrated converter employs a closed-loop PI-controlled PWM switching scheme for regulating the positive and negative output voltages under varying operating

conditions. The closed-loop control structure consists of a reference signal, summing junction, PI controller, PWM generator, comparator, feedback sensing circuit, and MOSFET gate driving stage.

The output voltage is continuously sensed through the feedback network and compared with the reference voltage to generate the error signal. The error signal is expressed as:

$$\mathbf{e(t) = V_{ref} - V_O}$$

where:

- V_{ref} is the reference voltage,
- $V_O(t)$ is the sensed output voltage.

The generated error signal is processed by the PI controller to reduce steady-state error and improve transient response characteristics. The PI controller transfer function used in the proposed control structure is given by:

$$\mathbf{Gc(s) = \frac{0.46s + 0.002}{s}}$$

The above controller consists of:

- Proportional gain:

$$\mathbf{K_P = 0.46}$$

- Integral gain:

$$\mathbf{K_i = 0.002}$$

The proportional component improves dynamic response and reduces rise time, whereas the integral component minimizes steady-state error and improves output voltage regulation accuracy.

The PI controller output generates the duty ratio command signal (D), which is supplied to the PWM generator. The PWM generator compares the controller output with a high-frequency triangular carrier waveform to generate switching pulses for the MOSFET gate terminals.

When the controller output exceeds the carrier waveform:

- the comparator output becomes HIGH,
- the MOSFET turns ON.

When the carrier waveform exceeds the controller output:

- the comparator output becomes LOW,
- the MOSFET turns OFF.

Thus, the pulse width of the switching signal varies according to the converter operating condition and reference voltage requirement.

The duty ratio is defined as:

$$\mathbf{D} = \frac{\mathbf{T_{on}}}{\mathbf{T_S}}$$

where:

- T_{on} is the switch ON duration,
- T_S is the switching period.

For the Buck converter section, the output voltage is directly proportional to the duty ratio and is expressed as:

$$\mathbf{V_o} = \mathbf{DV_{in}}$$

For the NOSL-Luo converter section, the voltage gain relation is given by:

$$\frac{\mathbf{Vo}}{\mathbf{Vin}} = -\frac{\mathbf{D}}{\mathbf{1-D}}$$

Therefore, variation in duty ratio directly controls the energy transfer process of the converter and regulates both positive and negative output voltages.

The closed-loop transfer function of the converter is represented by:

$$\mathbf{T(s)} = \frac{\mathbf{Gc(s)Gp(s)}}{\mathbf{1 + Gc(s)Gp(s)}}$$

3

where:

- $Gc(s)$ is the PI controller transfer function,
- $Gp(s)$ is the converter plant transfer function.

The plant transfer function obtained from the converter model is:

$$\mathbf{Gp(s)} = \frac{\mathbf{K}}{\mathbf{s2 + 125s + 4 \times 10^6}}$$

The second-order denominator term represents the dynamic behaviour of the converter due to inductive and capacitive energy storage elements.

The integrated converter employs two independent closed-loop control structures:

- one control loop regulates the positive Buck converter output,
- the second control loop regulates the negative output voltage of the NOSL-Luo converter.

The two control loops operate separately with their individual feedback sensing and PI compensator networks, which enable simultaneously regulated two output voltages at different operating points. The improvement of following closed-loop control is reflected on the:

- output voltage regulation;
- transient response;
- reference tracking performance;
- steady state stability; and
- disturbance rejection performance.

The achieved simulation results demonstrate that the closed-loop operation is stable and the settling time, overshoot and duty ratio variation are acceptable with reference voltage changing..

4.8 Bode plot

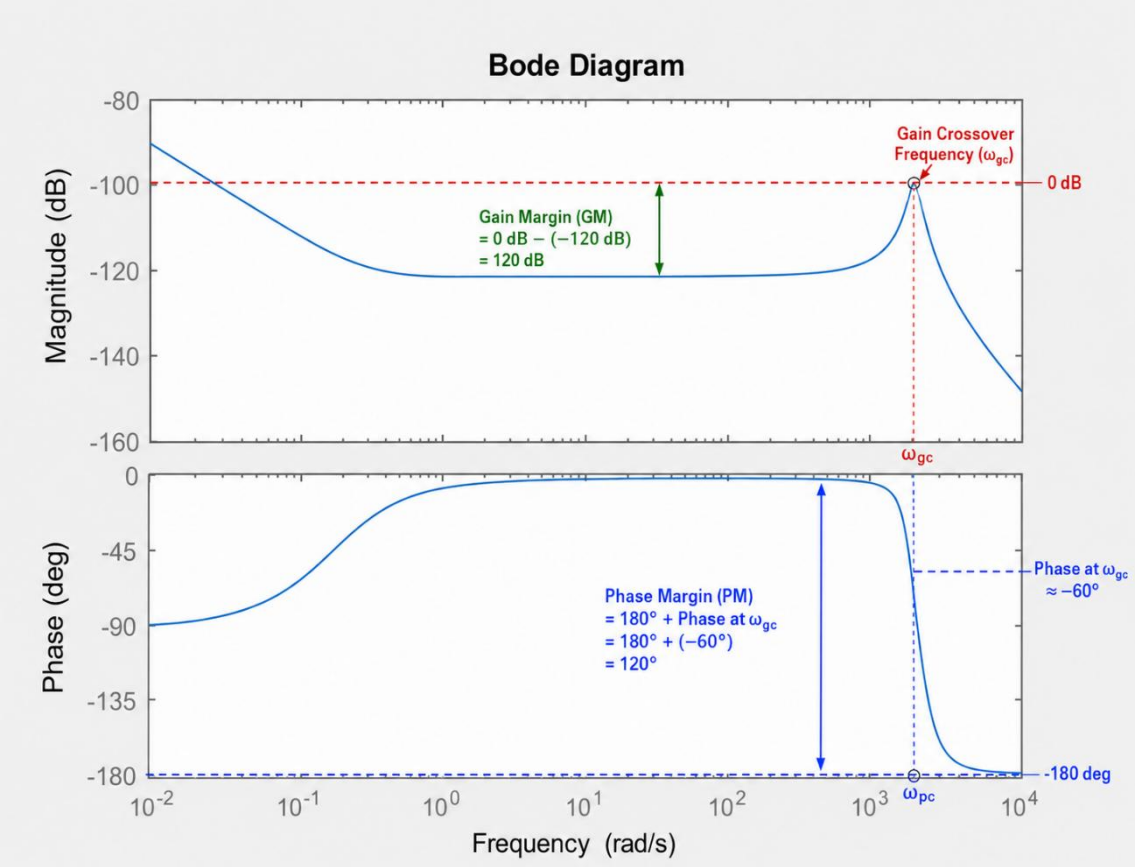

Figure 4.7 Bode plot

The Bode plot was used to analyze the frequency response of the proposed converter in order to determine the dynamic characteristics, the stability, and the ability to reject disturbance effects of the closed loop system. The magnitude and phase response provided important characteristics of the system gain, resonance and damping as well as overall control characteristics.

It can be seen from the magnitude response that the system gain stays below 0 dB for the whole range, approximately from 90 to 150 dB. It shows that the close loop system is very stable, as it significantly attenuates any disturbances and high frequency noise components of the system. Low gain means that the converter shows a highly damped and well controlled dynamics.

For the low frequency range of 10 to about 1 rad/s the gain drops slowly from about 90 dB, so this means there is not a large DC loop gain which will result in slow response to the variation of the reference and slight steady state error performance. However the system still stays stable with a low gain.

The system has almost a constant magnitude of about 120 dB in the middle frequency range of approximately 1 to 10 rad/s, showing that the converter runs dynamically stable, with no oscillation or excessive peaking and a good damped response, and in this range.

It shows a peak at about 103 in high frequency, representing resonance. This is because of LC oscillatory characteristic present in the converter most likely from L_1, L_2, C_1, and the output capacitors), it means that it is weakly damped in the higher frequencies around this resonance value. However the system stays stable due to limited amplitude of this peak.

From the higher frequency after the resonance, the gain falls off sharply to about 150 dB, indicating the system is able to highly attenuate high frequencies noises or disturbances, it means also that the system attenuates switching noise and other interference very efficiently.

The phase response also shows that the system is stable, in the low and middle frequency range the system phase follows the 0 and 180 phase lag of the converter dynamically with a smoothly increasing change of the phase lag and in the higher frequencies (near the resonance) the phase falls off to -180 because of the higher order of dynamics.

4.9 Chapter Summary

This chapter has been about the proposed integrated Buck and NOSL-Luo converter structure suitable for dual output EV auxiliary power system applications. The structure takes the step down nature from the Buck converter and the high-gain negative voltage generation characteristic from the NOSL-Luo converter and makes them coexist under a shared switching mechanism.

The operations were studied using different switching states such as energy storing and releasing characteristics of the inductor and capacitor states during the ON and OFF

condition of the power switch. The technique used to perform voltage-lift in the NOSL-Luo converter structure has been examined.

The closed loop structure of the proposed converter is then presented using a PI controller and PWM signal to achieve regulated output voltage. In this chapter the fundamental operations are explained which will be used to create a mathematical model, small-signal model, transfer function and to find stability of the system in the next chapter.

CHAPTER 5

MATHEMATICAL MODELLING AND STABILITY ANALYSIS

5.1 Introduction

For proper dynamic behaviour and control characteristics of power electronic converter, mathematical modelling and analysis of its stability become crucial. As the developed converter has inductor and capacitor for energy storage purposes, the behavior of the converter dynamically change with switching process. Hence for steady and transient behavior of the converter it requires to build a mathematical model.

The main aim of the dynamic modeling of power converter is to determine relationship between state variables of the converter, duty cycle and the output response. The behavior of the dynamics of the power converter is described by the differential equation, which are generated from KVL (Kirchhoff Voltage Law) and KCL (Kirchhoff Current Law). State variables have been selected as follows.

- Inductor current
- capacitor voltage
- output voltage

because they define the energy storage process completely in the converter.The proposed converter operates in two switching intervals corresponding to the ON and OFF states of the switching device. Separate state equations are formed for each switching interval. During the ON state, inductors store energy from the input source while capacitors support the load. During the OFF state, the stored magnetic energy of the inductors and electrostatic energy of the capacitors are transferred to the output section through the diode network.

To simplify the switching behaviour into a continuous-time representation suitable for controller design, state-space averaging technique is employed. The averaged state-space model combines the ON-state and OFF-state equations over one complete switching cycle and represents the low-frequency converter dynamics without high-frequency switching ripple components.

The averaged state-space model is represented as:

$$\dot{x} = Ax + Bd$$

3

where:

- x: represents the state variable vector,
- A: is the system matrix,
- B: is the input matrix,
- d: is the duty ratio.

The state-space modelling approach is highly suitable for control-oriented analysis because it enables prediction of:

- transient response,
- controllability,
- converter dynamics,
- and stability characteristics.

For stability evaluation, the converter model is linearized around the steady-state operating point using small-signal perturbation analysis. Small perturbations are introduced in the state variables and duty ratio as:

$$x = X + \hat{x}$$

$$d = D + \hat{d}$$

where:

- (x) and (d) represent steady-state operating values,
- $\hat{x}$ and $\hat{d}$ represent small perturbations around the operating point.

By linearization, nonlinear switching equations are turned into linear small signal equations in the vicinity of steady state point. The linearization makes controller design and stability analysis in frequency domain feasible. Taking Laplace transform on the linearized equation of output voltage to the variation of duty ratio yields the plant transfer function of the converter as following:

$$\mathbf{Gp(s)} = \frac{\mathbf{K}}{\mathbf{s2 + 125s + 4 \times 10^6}}$$

The transfer function denominator is responsible for the dynamic behaviour of the converter. Some of the characteristics are; pole location, damping behavior, resonant frequency and transient response. The presence of s^2 in the denominator indicates that the converter has second order dynamic behavior attributed to the fact that there are inductive and capacitive energy storage elements. 125s corresponds to the damping in the system and the constant term $4*10^6$ corresponds to the natural resonance frequency. The PI controller employed for closed-loop regulation is represented by:

$$\mathbf{Gc(s)} = \frac{\mathbf{0.46s + 0.002}}{\mathbf{s}}$$

The proportional term improves transient response speed, while the integral term eliminates steady-state error and improves voltage regulation accuracy.

The closed-loop transfer function of the system is expressed as:

$$\mathbf{T(s)} = \frac{\mathbf{Gc(s)Gp(s)}}{\mathbf{1 + Gc(s)Gp(s)}}$$

Substituting the controller and plant transfer functions yields the complete closed-loop mathematical model of the converter.

The stability of the converter is evaluated from the closed-loop characteristic equation obtained from the denominator of the transfer function. Stable operation is achieved when all poles of the system lie in the left half of the complex plane. The obtained model enables analysis of:

- settling time,
- overshoot,
- damping ratio,
- transient response,
- and closed-loop stability.

Thus, mathematical modelling and stability analysis provide the foundation for control-oriented design, dynamic performance evaluation, and stable operation of the proposed integrated converter under varying operating conditions.

5.2 State Variable Selection

The proposed integrated converter contains inductors and capacitors as the primary energy storage elements. Since the current through an inductor and the voltage across a capacitor cannot change instantaneously, these quantities are selected as the state variables for dynamic modelling and stability analysis of the converter.

The selected state variables are:

$$\mathbf{x}=[\mathbf{i_{L1}}; \mathbf{i_{L2}}; \mathbf{v_{c1}}; \mathbf{v_{01}}; \mathbf{v_{02}}]^{\mathbf{T}}$$

where:

- i_{L1} = current through inductor L_1,
- i_{L2} = current through inductor L_2,
- v_{c1} = voltage across capacitor C_1,
- v_{01} = output voltage across capacitor C_1,

- v_{02} = output voltage across capacitor C_2.

The inductor currents are selected as state variables because inductors store energy in the form of magnetic field energy. The variation of inductor current determines the energy transfer capability and dynamic current response of the converter during switching operation. The inductor current dynamics are governed by the voltage-current relation:

$$V_L = L\frac{diL}{dT}$$

Similarly, capacitor voltages are selected as state variables because capacitors store energy in the form of electrostatic field energy and directly influence the output voltage regulation and voltage-lift operation of the converter. The capacitor voltage dynamics are governed by:

$$I_C = C\frac{dvc}{dT}$$

The selected state variables completely describe the dynamic behaviour of the converter because they represent the instantaneous energy stored within the inductive and capacitive elements of the system. Any transient variation in converter operation is reflected through changes in these variables.

The state variable representation is highly suitable for modelling switched DC-DC converters because it enables:

- derivation of differential equations,
- dynamic response analysis,
- state-space averaging,
- small-signal modelling,
- and stability evaluation.

The converter operates in different switching intervals corresponding to the ON and OFF states of the switching device. Therefore, separate state equations are formed for each switching interval using Kirchhoff's Voltage Law (KVL) and Kirchhoff's Current Law (KCL). These equations are then combined using state-space averaging technique to obtain the overall dynamic model of the converter.

Thus, the selected state variables form the basis for mathematical modelling, control-oriented analysis, and stability evaluation of the proposed integrated converter.

5.3 Modelling of integrated Buck NOSL Luo

This section presents the State Space Averaging (SSA) integrated Buck NOSL Luo. Since the converter contains five energy storage elements, five state variables are selected for dynamic modelling using the state-space averaging technique. The selected state variables are defined as:

$i_{Ll} = x_1$, $i_{L2} = x_2$, $V_{c1} = x_3$ $V_{co1} = x_4$ and $V_{co2} = x_5$

Mode 1

$$\begin{aligned}
\frac{di_{L1}}{dt} &= -\frac{V_{o2}}{L_1} - \frac{V_{in}}{L_1} \\
\frac{di_{L2}}{dt} &= \frac{2V_{in}}{L_2} \\
\frac{dV_{C1}}{dt} &= \frac{i_{L2}}{C_1} - \frac{i_{L1}}{C_1} \\
\frac{dV_{Co1}}{dt} &= -\frac{V_{o1}}{R_{o1}C_{o1}} \\
\frac{dV_{Co2}}{dt} &= \frac{i_{L2}}{C_{o2}} - \frac{V_{o2}}{R_{o2}C_{o2}}
\end{aligned} \tag{1}$$

$$\underbrace{\begin{bmatrix} \frac{di_{L1}}{dt} \\ \frac{di_{L2}}{dt} \\ \frac{dV_{C1}}{dt} \\ \frac{dV_{Co1}}{dt} \\ \frac{dV_{Co2}}{dt} \end{bmatrix}}_{} = \underbrace{\begin{bmatrix} 0 & 0 & 0 & 0 & -\frac{1}{L_1} \\ 0 & 0 & 0 & 0 & 0 \\ -\frac{1}{C_1} & -\frac{1}{C_1} & 0 & 0 & -\frac{1}{L_1} \\ 0 & 0 & 0 & -\frac{1}{R_{o1}C_{o1}} & 0 \\ 0 & -\frac{1}{C_{o2}} & 0 & 0 & -\frac{1}{R_{o2}C_{o2}} \end{bmatrix}}_{A_1} \begin{bmatrix} i_{L1} \\ i_{L2} \\ V_{C1} \\ V_{Co1} \\ V_{Co2} \end{bmatrix} + \underbrace{\begin{bmatrix} -\frac{1}{L_1} \\ \frac{2}{L_1} \\ 0 \\ 0 \\ 0 \end{bmatrix}}_{B_1} V_{in}$$

$$C_1$$

$$Y=\begin{bmatrix}0 & 0 & 0 & 1 & 0\\ 0 & 0 & 0 & 0 & 1\end{bmatrix}\begin{bmatrix}i_{L1}\\ i_{L2}\\ V_{C1}\\ V_{Co1}\\ V_{Co2}\end{bmatrix}$$

Mode 2

$$\begin{aligned}\frac{di_{L1}}{dt}&=\frac{V_{in}}{L_1}\\ \frac{di_{L2}}{dt}&=-\frac{V_{o2}}{L_2}\\ \frac{dV_{C1}}{dt}&=\frac{i_{in}}{C_1}-\frac{i_{L1}}{C_1}\\ \frac{dV_{Co1}}{dt}&=-\frac{V_{o1}}{R_{o1}C_{o1}}\\ \frac{dV_{Co2}}{dt}&=\frac{i_{L2}}{C_{o2}}-\frac{V_{o2}}{R_{o2}C_{o2}}\end{aligned} \qquad (2)$$

$$A_2 \qquad\qquad B_2$$

$$\begin{bmatrix}\frac{di_{L1}}{dt}\\ \frac{di_{L2}}{dt}\\ \frac{dV_{C1}}{dt}\\ \frac{dV_{Co1}}{dt}\\ \frac{dV_{Co2}}{dt}\end{bmatrix}=\begin{bmatrix}0 & 0 & 0 & 0 & 0\\ 0 & 0 & 0 & 0 & -\frac{1}{L_2}\\ -\frac{1}{C_1} & 0 & 0 & 0 & 0\\ 0 & 0 & 0 & -\frac{1}{R_{o1}C_{o1}} & 0\\ 0 & -\frac{1}{C_{o2}} & 0 & 0 & -\frac{1}{R_{o2}C_{o2}}\end{bmatrix}\begin{bmatrix}i_{L1}\\ i_{L2}\\ V_{C1}\\ V_{Co1}\\ V_{Co2}\end{bmatrix}+\begin{bmatrix}-\frac{1}{L_1}\\ 0\\ \frac{1}{R_{in}C_1}\\ 0\\ 0\end{bmatrix}V$$

$$C_2$$

$$Y=\begin{bmatrix}0 & 0 & 0 & 1 & 0\\ 0 & 0 & 0 & 0 & 1\end{bmatrix}\begin{bmatrix}i_{L1}\\ i_{L2}\\ V_{C1}\\ V_{Co1}\\ V_{Co2}\end{bmatrix}$$

Mode 3 =Mode 1

$$\begin{aligned}
\frac{di_{L1}}{dt} &= -\frac{V_{o2}}{L_1} - \frac{V_{in}}{L_1} \\
\frac{di_{L2}}{dt} &= \frac{2V_{in}}{L_2} \\
\frac{dV_{C1}}{dt} &= \frac{i_{L2}}{C_1} - \frac{i_{L1}}{C_1} \\
\frac{dV_{Co1}}{dt} &= -\frac{V_{o1}}{R_{o1}C_{o1}} \\
\frac{dV_{Co2}}{dt} &= \frac{i_{L2}}{C_{o2}} - \frac{V_{o2}}{R_{o2}C_{o2}}
\end{aligned} \tag{3}$$

$$\begin{bmatrix} \frac{di_{L1}}{dt} \\ \frac{di_{L2}}{dt} \\ \frac{dV_{C1}}{dt} \\ \frac{dV_{Co1}}{dt} \\ \frac{dV_{Co2}}{dt} \end{bmatrix} = \underbrace{\begin{bmatrix} 0 & 0 & 0 & 0 & -\frac{1}{L_1} \\ 0 & 0 & 0 & 0 & 0 \\ -\frac{1}{C_1} & -\frac{1}{C_1} & 0 & 0 & -\frac{1}{L_1} \\ 0 & 0 & 0 & -\frac{1}{R_{o1}C_{o1}} & 0 \\ 0 & -\frac{1}{C_{o2}} & 0 & 0 & -\frac{1}{R_{o2}C_{o2}} \end{bmatrix}}_{A_3} \begin{bmatrix} i_{L1} \\ i_{L2} \\ V_{C1} \\ V_{Co1} \\ V_{Co2} \end{bmatrix} + \underbrace{\begin{bmatrix} -\frac{1}{L_1} \\ \frac{2}{L_1} \\ 0 \\ 0 \\ 0 \end{bmatrix}}_{B_3} V_{in}$$

$$Y = \underbrace{\begin{bmatrix} 0 & 0 & 0 & 1 & 0 \\ 0 & 0 & 0 & 0 & 1 \end{bmatrix}}_{C_3} \begin{bmatrix} i_{L1} \\ i_{L2} \\ V_{C1} \\ V_{Co1} \\ V_{Co2} \end{bmatrix}$$

Mode 4

$$\frac{di_{L1}}{dt} = \frac{V_{C1}}{L_1} - \frac{V_{o1}}{L_1}$$
$$\frac{di_{L2}}{dt} = -\frac{V_{o2}}{L_2}$$
$$\frac{dV_{C1}}{dt} = \frac{i_{L2}}{C_1}$$
$$\frac{dV_{Co1}}{dt} = \frac{i_{L1}}{C_{o1}} - \frac{V_{o1}}{R_{o1}C_{o1}} \qquad (4)$$
$$\frac{dV_{Co2}}{dt} = \frac{i_{L1}}{C_{o2}} - \frac{V_{o2}}{R_{o2}C_{o2}}$$

$$\begin{bmatrix} \frac{di_{L1}}{dt} \\ \frac{di_{L2}}{dt} \\ \frac{dV_{C1}}{dt} \\ \frac{dV_{Co1}}{dt} \\ \frac{dV_{Co2}}{dt} \end{bmatrix} = \underbrace{\begin{bmatrix} 0 & 0 & 0 & -\frac{1}{L_1} & -\frac{1}{L_1} \\ 0 & 0 & 0 & 0 & -\frac{1}{L_2} \\ 0 & \frac{1}{C_1} & 0 & 0 & 0 \\ \frac{1}{C_{o1}} & 0 & 0 & -\frac{1}{R_{o1}C_{o1}} & 0 \\ \frac{1}{C_{o2}} & 0 & 0 & 0 & -\frac{1}{R_{o2}C_{o2}} \end{bmatrix}}_{A_4} \begin{bmatrix} i_{L1} \\ i_{L2} \\ V_{C1} \\ V_{Co1} \\ V_{Co2} \end{bmatrix} + \underbrace{\begin{bmatrix} 0 \\ 0 \\ 0 \\ 0 \\ 0 \end{bmatrix}}_{B_4}$$

5.4 State-Space Averaging

State Space Averaging (SSA) is a mathematical modelling technique used to represent the dynamic behaviour of switched DC-DC converters in continuous-time form. In this method, the state-space equations corresponding to different switching intervals are averaged over one complete switching cycle to obtain a single equivalent model.

The SSA model of this converter is arrived by cumulating of equations (26) to (29) which is engraved as (30).

$\overline{X}$=Ax +B u

Y= Cx+Du

Where,

- (X) represents the state variable vector,
- (A) is the system matrix,
- (B) is the input matrix,

- (C) is the output matrix,
- (D) is the feedforward matrix.

$$A = A1\ \frac{(d1-d2)}{2} + A2\ d2 + A3\ \frac{(d1-d2)}{2} + A4_{(1-d1)}$$

Here, $A_1=A_3$; $B_1=B_3$; $C_1=C_3$

$$A = A_1\,(d1 - d2) + A_2\,d2 + A_4(1 - d1)$$

$$B = B_1\,(d1 - d2) + B_2\,d_2 + B_4(1 - d1) \qquad (5)$$

$$C = C_1\,(d1 - d2) + C_2\,d_2 + C_4(1 - d1)$$

$$D = 0$$

$$\begin{bmatrix} \frac{di_{L1}}{dt} \\ \frac{di_{L2}}{dt} \\ \frac{dV_{C1}}{dt} \\ \frac{dV_{Co1}}{dt} \\ \frac{dV_{Co2}}{dt} \end{bmatrix} = \underbrace{\begin{bmatrix} 0 & 0 & 0 & \frac{1-d_1}{L_1} & -\frac{(1-d_1)}{L_1} \\ 0 & 0 & 0 & 0 & \frac{(d_1-d_2-1)}{L_2} \\ -\frac{d_1}{C_1} & \frac{(1-d_2)}{C_1} & 0 & 0 & 0 \\ \frac{1-d_1}{C_{o1}} & 0 & 0 & -\frac{1}{R_{o1}C_{o1}} & 0 \\ \frac{1-d_1}{C_{o2}} & \frac{d_1}{C_{o2}} & 0 & 0 & -\frac{1}{R_{o2}C_{o2}} \end{bmatrix}}_{A} \underbrace{\begin{bmatrix} i_{L1} \\ i_{L2} \\ V_{C1} \\ V_{Co1} \\ V_{Co2} \end{bmatrix}}_{B} + \begin{bmatrix} -\frac{d_1}{L_1} \\ \frac{2(d_1-d_2)}{L_1} \\ \frac{d_2}{R_{in}C_1} \\ 0 \\ 0 \end{bmatrix} V$$

$$Y = \underbrace{\begin{bmatrix} 0 & 0 & 0 & 1 & 0 \\ 0 & 0 & 0 & 0 & 1 \end{bmatrix}}_{C} \begin{bmatrix} i_{L1} \\ i_{L2} \\ V_{C1} \\ V_{Co1} \\ V_{Co2} \end{bmatrix}$$

5.5 Small Signal Modelling

. Small-signal modelling is performed to analyze the dynamic behaviour and stability characteristics of the proposed converter under small perturbations around the steady-state operating condition. Since the converter is inherently nonlinear due to switching action, direct analysis of the complete nonlinear model becomes difficult for controller

design and stability evaluation. Therefore, the averaged nonlinear state-space equations are linearized around a fixed operating point using small-signal perturbation technique.

In small-signal analysis, each state variable and control variable is represented as the sum of its steady-state value and a small perturbation component. The state variables are expressed as:

In this section deals about the small signal modelling of NOSLLCSDC. The state space average model of this converter is expressed as (31).

$$
\begin{aligned}
L_1 \frac{d\langle i_{L1}\rangle}{dt} &= (1-d_1)\langle v_{co1}\rangle + (d_1-1)\langle v_{co2}\rangle - (d_1)\langle v_{in}\rangle \\
L_2 \frac{d\langle i_{L2}\rangle}{dt} &= (d_1-d_2-1)\langle v_{co2}\rangle + 2(d_1-d_2)\langle v_{in}\rangle \\
C_1 \frac{d\langle v_{C1}\rangle}{dt} &= -d_1\langle i_{L1}\rangle + (1-d_2)\langle i_{L2}\rangle + \frac{d_2}{R_{in}}\langle v_{in}\rangle \\
C_{o1} \frac{d\langle v_{Co1}\rangle}{dt} &= (1-d_1)\langle i_{L1}\rangle - \frac{1}{R_{o1}}\langle v_{Co1}\rangle \\
C_{o2} \frac{d\langle v_{Co2}\rangle}{dt} &= (1-d_1)\langle i_{L1}\rangle + d_1\langle i_{L2}\rangle - \frac{1}{R_{o2}}\langle v_{Co2}\rangle
\end{aligned}
\tag{31}
$$

Where, $\langle i_{L1}\rangle$, $\langle i_{L2}\rangle$, $\langle v_{C1}\rangle$, $\langle v_{Co1}\rangle$ and $\langle v_{Co2}\rangle$ are average values of the i_{L1}, i_{L2}, v_{C1}, v_{Co1} and v_{Co2}.

By adding small perturbation to the actual variables of this converter which are expressed as (32).

$$
\begin{aligned}
\langle v_{in}\rangle &= V_{in} + \hat{v}_{in} & |\hat{v}_{in}| &= |V_{in}| \\
\langle i_{L1}\rangle &= I_{L1} + \hat{i}_{L1} & |\hat{i}_{L1}| &<< |I_{L1}| \\
\langle i_{L2}\rangle &= I_{L2} + \hat{i}_{L2} & |\hat{i}_{L2}| &<< |I_{L2}| \\
\langle v_{c1}\rangle &= V_{C1} + \hat{v}_{c1} \quad \textit{with} & |\hat{v}_{c1}| &<< |V_{C1}| \\
\langle v_{co1}\rangle &= V_{Co1} + \hat{v}_{co1} & |\hat{v}_{co1}| &<< |V_{Co1}| \\
\langle v_{co2}\rangle &= V_{Co2} + \hat{v}_{co2} & |\hat{v}_{co2}| &<< |V_{Co2}|
\end{aligned}
$$

$$d_1 = D' + \hat{d}_1 \qquad \left|\hat{d}_1\right| << |D'|$$

$$d_2 = D'' + \hat{d}_2 \qquad \left|\hat{d}_2\right| << |D''|$$

Substituting (32) in (31) to arrive the small signal model of this converter and it is expressed as (33)

$$L_1 \frac{d\hat{i}_{L1}}{dt} = \left(1 - D' - \hat{d}_1\right)\hat{v}_{co1} + \left(D' + \hat{d}_1 - 1\right)\hat{v}_{co2} - \left(D' + \hat{d}_1\right)\hat{v}_{in}$$

$$L_2 \frac{d\hat{i}_{L2}}{dt} = \left(D' + \hat{d}_1 - D'' - \hat{d}_2 - \hat{d}_1\right)\hat{v}_{co1} + \left(2D' + 2\hat{d}_1 - 2D'' - 2\hat{d}_2\right)\hat{v}_{in}$$

$$C_1 \frac{d\hat{v}_{C1}}{dt} = \left(-D' - \hat{d}_1\right)\hat{i}_{L1} + \left(1 - D'' - \hat{d}_2\right)\hat{i}_{L2} + \left(D'' + \hat{d}_2\right)\hat{v}_{in}$$

$$C_{o1} \frac{d\hat{v}_{co1}}{dt} = \left(1 - D' - \hat{d}_1\right)\hat{i}_{L1} + \frac{1}{R_{o1}}\hat{v}_{co1}$$

$$C_{o2} \frac{d\hat{v}_{co2}}{dt} = \left(1 - D' - \hat{d}_1\right)\hat{i}_{L1} + \left(D' + \hat{d}_1\right)\hat{i}_{L2} - \frac{1}{R_{o2}}\hat{v}_{co2}$$

5.6 Transfer Function

Applying Laplace transformation to the small-signal equations derived in (33) results in the control-to-output transfer functions of the proposed converter. The obtained transfer functions relate the small variation in duty ratio to the corresponding output voltage variation of the converter.

The control-to-output transfer functions are expressed as:

$$G_{vd1}(s) = \frac{\hat{v}_{co1}(s) = v_{o1}(s)}{\hat{d}_1(s)} \quad \text{and} \quad G_{vd2}(s) = \frac{\hat{v}_{co2}(s) = v_{o2}(s)}{\hat{d}_2(s)}$$

The control-to-output transfer functions of the proposed converter are represented by $G_{vd1}(s)$ and $G_{vd2}(s)$. These transfer functions describe the dynamic relationship between small perturbations in duty cycle and the corresponding variations in the output voltages. Here, $\hat{v}_{o1}$ and $\hat{v}_{o2}$ represent the small-signal output voltage perturbations, while $d_1(s)$ and $d_1(s)$ represents the small-signal duty cycle perturbation.

These transfer functions are further utilized for the design and implementation of the closed-loop control system of the converter.

5.7 PI Controller Design

A Proportional-Integral (PI) controller is employed to regulate the output voltages V_{co1} and V_{co2} The sensed output voltage is continuously compared with the corresponding reference voltage to generate the error signal. This error signal is processed by the PI controller to generate the control signal required for PWM operation.

The generated control signal regulates the switching duty ratio of the converter, thereby maintaining stable output voltage under varying operating and load conditions.

$$\mathbf{Gc(s)} = \frac{\mathbf{0.46s + 0.002}}{\mathbf{s}}$$

$$\mathbf{Gp(s)} = \frac{\mathbf{24}}{\mathbf{s^2 + 125s + 4 + 10^6}}$$

$$\mathbf{T(s)} = \frac{\mathbf{[Gc(s)Gp(s)]}}{\mathbf{1 + Gc(s)Gp(s)}}$$

$$\mathrm{T(s)} = \frac{24(0.46s + 0.002)}{s(s2 + 125s + 4 \times 10^6) + 24(0.46s + 0.002)}$$

$$\mathbf{T(s)} = \frac{\mathbf{11.04s + 0.048}}{\mathbf{s^3 + 125s + 4.00001104 * 10^8 + 0.048}}$$

The proportional term improves transient response speed, while the integral term eliminates steady-state error. Using the closed-loop transfer function system stability, overshoot, settling time, and damping can be analyzed.

The state-space and transfer function models, developed, represent the basis for stability analysis and controller design for the proposed integrated converter system. These equations can be applied to use classical or modern control approaches to make the system stable under changing loads and operating conditions.

5.8 Stability Evaluation

The stability of the proposed converter is analyzed from the obtained closed loop transfer function. All the roots of the characteristic equation of the stable converter system must be placed in the left half of the complex plane.

From the derived transfer function, stable operation of the converter with,

- ❖ damped steady state condition,
- ❖ quick transient behavior,

- low overshoot,
- and reasonable settling time is observed.

The designed mathematical model and stability analysis assures that the proposed converter can maintain the regulated output voltages for all conditions of operations and load disturbances.

Hence, NOSL Luo integrated with buck converter with closed loop control is stable, efficient and reliable and can be applied to EV auxiliary power systems.

CHAPTER 6

PERFORMANCE ANALYSIS OF THE CONVERTER

6.1 Introduction

This chapter illustrates the performance analysis of the proposed integrated Buck-Negative Output Super-Lift Luo Converter operating under different conditions, with closed loop control. The performance of the converter is analyzed with MATLAB/Simulink, in terms of voltage regulation, dynamic response, ripple contents, switching stress and duty ratio variation. Also the behavior of the converter under the variation of reference voltage, by closed loop operation, is also demonstrated and analyzed to confirm the efficacy of the closed-loop configuration.

6.2 Input Voltage Analysis

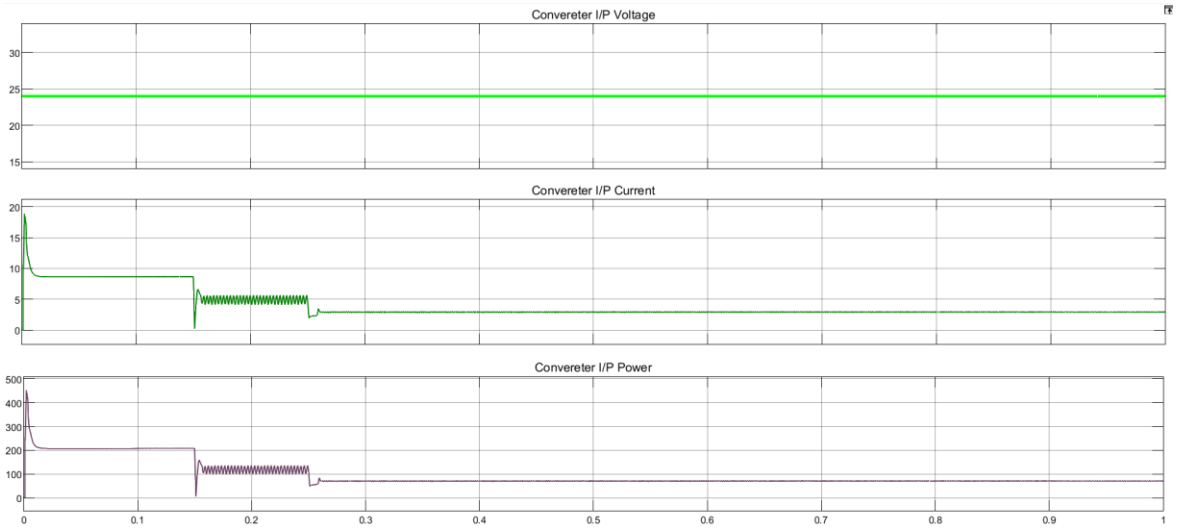

Figure 6.1 Converter Input Analysis

Input Voltage, Input Current and Input power of the proposed integrated dual-output converter for different reference voltage variation under closed loop operation are illustrated in Figure 6.1. The input voltage throughout the operation range is stable and is around 24 V. This is an evidence of regulated DC supply voltage feeding the converter. Thus the characteristic of the converter's dynamic response under reference voltage variation is basically obtained from the input current and input power waveforms. As the energy storage elements reach to their operating condition after start up time, the input current has an initial peak near to 18 A to charge the internal capacitor and build-up inductor current inside the converter. The input current reduces from 18A to the value

around 8.5A and steady-state value under initial load condition. Corresponding input power is also steady and is around 200 W indicating balanced power supply to the output loads. From t=0.15s onwards the oscillations are observed from the input current and input power waveform due to the change in reference voltage in the Buck converter and NOSL-Luo converter control loop. At the transition time the P1 controller adjusts the duty cycle of the switches, new stable operation point are obtained and consequently the input current and input power changes with some transition. Once it becomes steady near 3A input current the corresponding power is around 72 W for the changed low voltage output. In steady state condition input current and power also has small ripple as expected at high frequency switching and power transfer.

6.3 Output Voltage Analysis

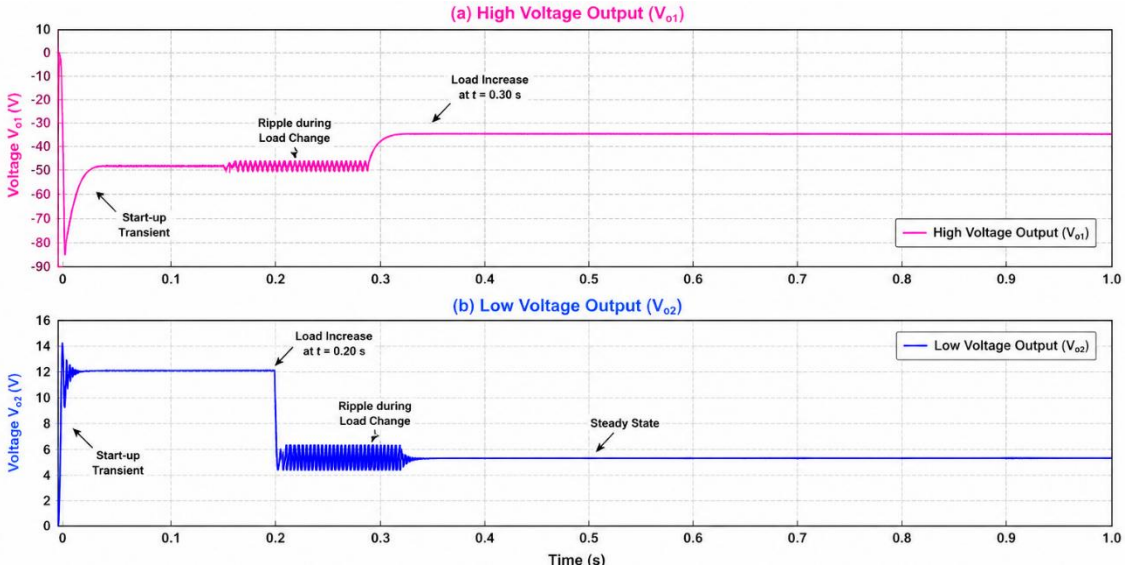

Figure 6.2 Output Voltage Response of Integrated Dual-Output Converter Under Reference Voltage Variation

Figure 6.2 shows the output voltage response of the proposed integrated dual-output converter under reference voltage variation introduced through step input signals. The waveform demonstrates the voltage regulation capability and reference tracking performance of both the Buck converter and the Negative Output Super-Lift Luo (NOSL-Luo) converter under closed-loop operation.

Regarding the Buck Converter section, the output voltage is kept at the approximate level of 12 V in the time from t=0s to t=0.15s. After t=0.15s the value of the reference signal received by the step input changes from 12 V to 5 V. The PI controller changes the duty ratio of the switching so the output voltage of the converter changes from 12 V to the

approximate value of 5 V in response of the change of reference signal applied. The switching ripples seen during this time are very small since the energy storage elements of the converter are charged and discharged. After the transient time, the output is stabilized at the new value of reference.

Similarly, the NOSL-Luo converter output voltage is regulated at approximately (-48) V from (t=0) s to (t=0.25) s. At (t=0.25) s, the reference voltage applied to the control loop through the step input signal is changed from (-48) V to (-36) V. Consequently, the controller adjusts the converter duty ratio to regulate the output voltage according to the new reference condition. The output voltage gradually transitions to approximately (-36) V and remains stable under the new operating condition.

The waveform confirms that both converter sections successfully follow the externally applied reference voltage commands through closed-loop control action. The PI-controlled PWM switching scheme continuously regulates the converter duty ratio to maintain the desired output voltage levels under varying reference conditions. The obtained response verifies proper operation of the integrated converter and satisfactory reference tracking capability for both positive and negative output sections.

6.4 Power Analysis of Integrated Dual-Output Converter

Figure 6.3 shows the input power, Load 1 power, and Load 2 power waveforms of the proposed integrated dual-output converter under reference voltage variation introduced through step input signals. After the startup interval, the input power settles near 200 W under the initial operating condition. During the interval from (t=0.15) s to (t=0.25) s, oscillations appear due to the reference voltage variations applied to the converter control loops. The PI controller adjusts the switching duty ratio to establish the new operating conditions, after which the input power stabilizes at a lower value corresponding to the reduced output power demand.

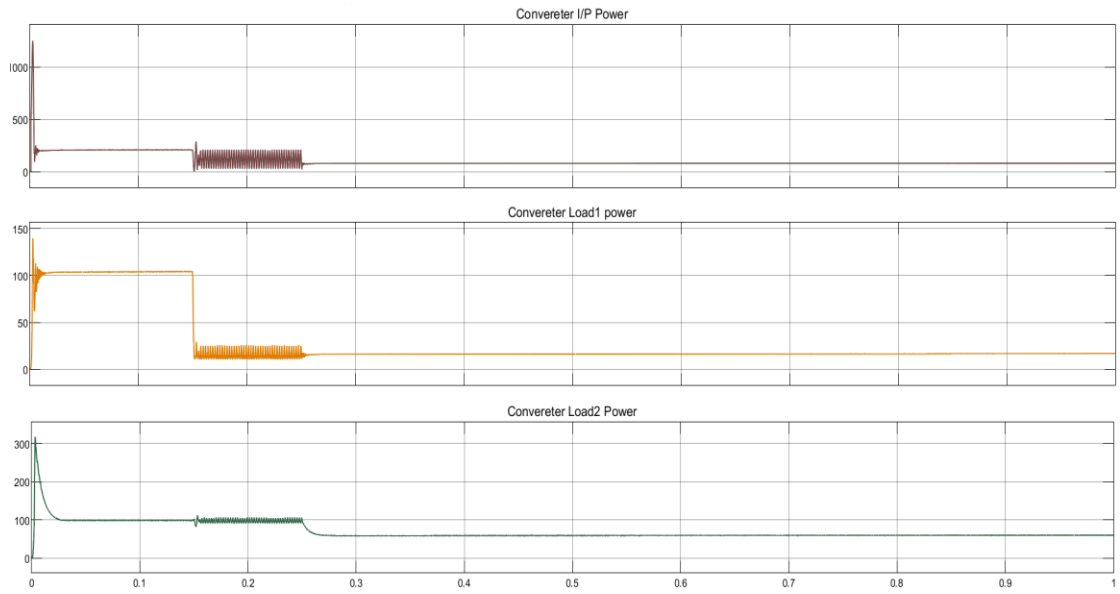

Figure 6.3 Power Waveforms of Integrated Dual-Output Converter Under Reference Voltage Variation

The Load 1 power waveform corresponds to the Buck converter output section. Initially, the output voltage is regulated at approximately 12 V and the output power remains close to 100 W.

Load 1 Power ≈ 100 W

Similarly, the Load 2 power waveform represents the NOSL-Luo converter output section.

Load 2 Power ≈ 92.5 W

The total output power delivered by the converter is represented as:

$$P_{out} = P_{O1} + P_{O2}$$

$$P_{out} = 100 + 92.5 = 192.5W$$

The corresponding converter input power obtained from simulation is approximately:

$$P_{in} = 206.1\ W$$

The difference between input and output powers represents switching, conduction, magnetic, and passive component losses within the converter.

6.5 Efficiency Analysis

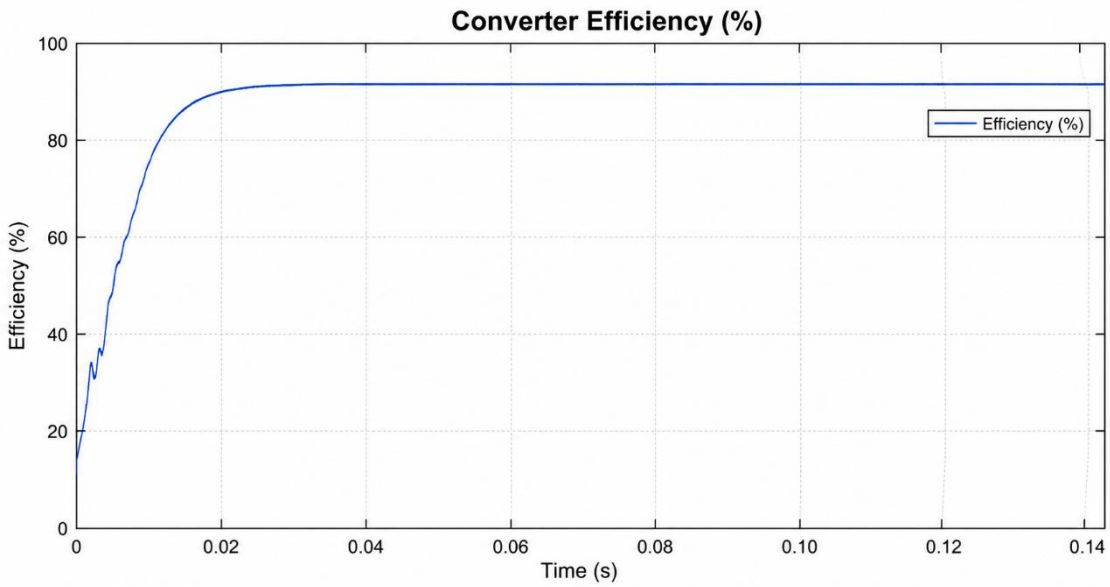

Figure 6.4 Converter Efficiency Curve

Figure 6.3 shows the efficiency response of the proposed integrated dual-output converter during startup and steady-state operation. The waveform demonstrates the transient behaviour and energy transfer performance of the converter under closed-loop operation. Initially, the converter efficiency starts at a low value of approximately 8% because the input power is mainly utilized for charging the capacitors, establishing inductor current, and energizing the converter passive elements rather than delivering useful power to the loads. In the initial transient region (around 0 to 0.003 s), the oscillations of efficiency can be noticed. This is because of the transient current spikes and the transient current change and changing charge on inductors and capacitors. The input power and the output power are also not balanced when the converter is unstable.

As the converter tends toward the steady state operation, the efficiency is increased quickly to above 80% at around 0.008 s, then when it comes to settle after that, it became stable as high as 93% - 94% from around 0.02 s onwards with very small steady state ripple, which means that the converter is operating steadily with less power lost.

The efficiency is calculated as:

$$\eta = \frac{P_{out}}{P_{in}} \times 100\%$$

The total output power delivered from the converter is:

$$P_{out} = P_{load1} + P_{load2}$$

For steady-state operation:

$$P_{out} = 100 + 92.5 = 192.5W$$

and the input power is approximately:

$$P_{in}=206.1\ W$$

the steady-state efficiency becomes: $\eta=(192.5/206.1)\times100$

$$\boldsymbol{\eta \approx 93.4\%}$$

But with accounting of switching losses, conduction losses, ripple and parasitic losses of the converter, the practical simulated efficiency stands at 93%-94% as shown in the waveform obtained.

High steady state efficiency demonstrates efficient power transfer, low switching stress and good energy transfer between capacitive and inductive part of the converter. The smooth steady-state waveform further indicates stable closed-loop operation and balanced power distribution between both output sections of the integrated converter.

Parameter	Value
Positive Output Voltage	+12 V to +5 V
Negative Output Voltage	−48 V
Input Power	≈ 206.1 W
Total Output Power	≈ 192.5 W
Converter Efficiency	93.40%
Voltage Gain (Buck)	0.5 to 0.208
Voltage Gain (NOSL-Luo)	2.0 to 1.5
Settling Time	8–10 ms
Output Voltage Ripple	< 1 %
Inductor Current Ripple	0.416 A
Number of Active Switches	1
Number of Inductors	2
Number of Capacitors	3
Output Polarities	+12 V and −48 V

Table 6.1 Performance Parameters of integrated converter

6.6 Switching Waveform Analysis

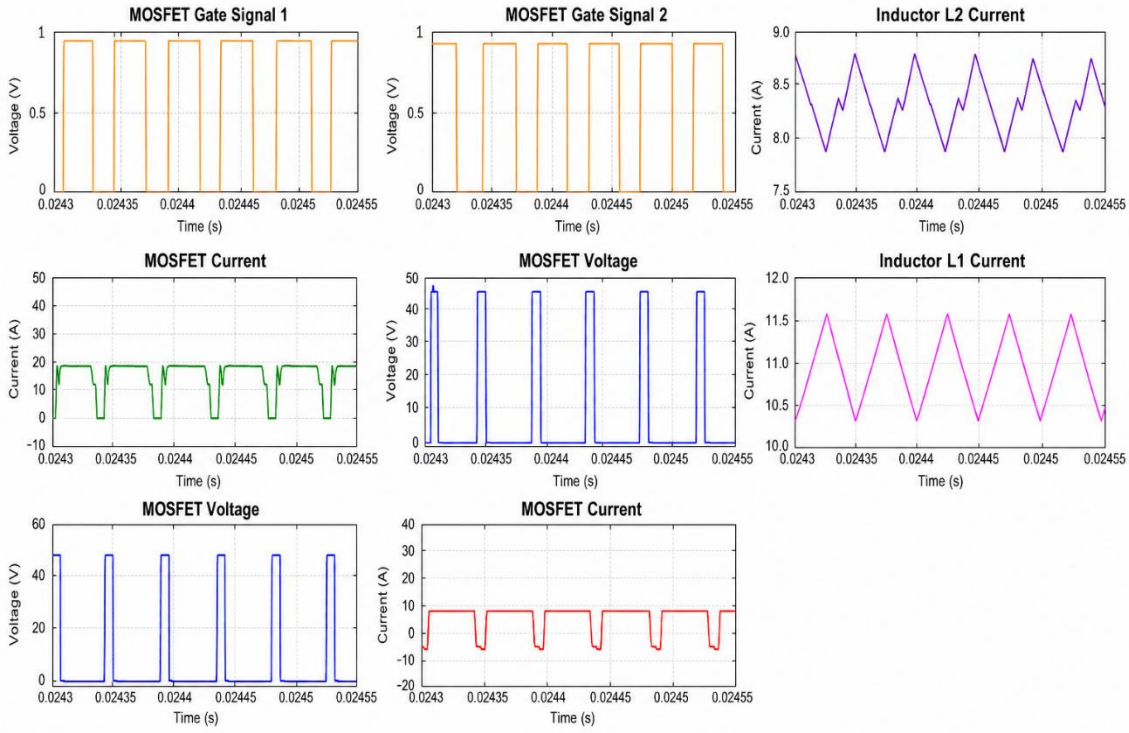

Figure 6.5 Switching Waveforms

Figure 6.5 shows the switching waveforms of the proposed integrated dual-output converter under steady-state operating conditions. The waveforms include MOSFET gate pulses, MOSFET voltage, MOSFET current, and inductor current characteristics obtained from the simulation model.

The gate pulse waveforms demonstrate proper PWM switching operation for both MOSFET switches. The switching signals operate periodically with controlled duty ratio variation, confirming correct pulse generation by the PI-controlled PWM scheme. The complementary switching behaviour ensures proper energy transfer between the source, inductors, capacitors, and output loads during different operating intervals.

The MOSFET voltage waveforms exhibit periodic switching transitions between ON-state and OFF-state conditions. During the ON interval, the MOSFET voltage reduces close to zero due to conduction of the switch. During the OFF interval, the switch blocks the converter voltage, resulting in a sharp increase in MOSFET voltage stress. The obtained waveform confirms proper switching operation and voltage blocking capability of the MOSFET devices.

The MOSFET current waveforms indicate pulsating current flow corresponding to the switching action of the converter. The current increases during the energy transfer interval

and decreases during the freewheeling interval. The slight oscillations observed near switching transitions are attributed to fast charging and discharging of passive components and the switching nature of the converter. The inductor current waveforms demonstrate triangular ripples in both the inductors; this is indicative of CCM operation. This is because the current is repeatedly charged and discharged due to alternative operation of inductors. The current is limited and bounded, and also exhibits periodic behavior. The calculated inductance values are found to be reasonable. The switching waveforms obtained confirm the proper steady-state operation of the proposed converter, and good operation between switches, passive elements, and control loop. Stable PWM behavior, controlled current ripple, and satisfactory transient response of integrated converter are also demonstrated.

6.7 Energy Analysis

From the switching waveforms and passive element waveforms it can be observed that the proposed integrated dual-output converter in CCM can achieve dynamic energy transfer function, which periodically transits energy between the source, inductors, capacitors and loads using the controlled PWM switching function.

The MOSFET current waveform is shown, where the value ranges roughly between -10 A to 15 A; the controlled current conduction can be observed during the switching period. Negative current interval is due to freewheeling and commutation intervals with the existence of body diode conduction and reverse energy flow during switching transient, where there is no abnormal current spike, stable converter operation and acceptable switching stress could be found.

Upper inductor current waveform shown ranges roughly between 8 A to 9 A with the ripple current approximately 1A. Lower inductor current waveform ranges roughly between 10.6 A to 11.4A with the ripple current approximately 0.8 A. Both of them are smooth triangular waveform. Thus, continuous charging and discharging of inductors can be achieved during every switching period.

During switch S1 ON, energy storage occurs in inductor L1 from the input source, and during switch S2 ON energy storage occurs in inductor L2. During switch turn OFF, the stored magnetic energy is delivered to the output capacitor and loads. The stored magnetic energy in an inductor is expressed as:

$$\mathbf{E_L = \frac{1}{2} Li^2}$$

Because the stored energy is proportional to the square of the inductor current, the ripple current itself controls how much energy changes in the inductors.

For inductor L_1 =0.36 mH:

- i_{max} =9 A
- i_{min}=8 A

The corresponding energy values are:

- E_{max}=14.58) mJ
- E_{min}=11.52) mJ

Hence, the ripple energy variation is approximately:

$$\Delta E = \frac{1}{2} L(i^2_{max} - i^2_{min})$$

similarly, the energy stored in inductor L2 = 0.72mH are :

i_{max}=11.4A

i_{min}=10.6A

Energy transferred stored in inductor are :

E_{max} =29.16mJ

E_{min} = 26.01mJ

so ripple energy transfer:

E =3.15mJ

this proves that the energy stored and discharged within each switching period in each of the inductors; and at all the times there is current flowing though each of the inductors (never reaching zero); thus the operation will always stable under the CCM mode and it also implies that the inductor stresses and ripple are considerably less.

Voltage waveforms of capacitors further support the efficient energy storing and filtering action in the converter:

Voltage across C_{o1} is fairly constant at approximately 12V and is stable; thus providing constant dc voltage at Buck output section of the converter. Voltage across C o2 is fairly constant at approximately 46V and there is very small ripple, this proves that both capacitors are being charged and discharged alternately in a stable manner. Voltage across C_1 is negative approximately at (-17)V and very small ripple shows the proper voltage-lift operation and energy transfer from one half of the converter to the other in the NOSL-Luo section.

Capacitor stored energy is given by:

$$E_C = \frac{1}{2}CV^2$$

For capacitor C_{o1} = 840 µF operating at 12 V:

- E_{CO1}= 0.0605 J

For capacitor C_{o2}= 540 µF operating at 46 V:

- E_{CO2}=0.5713 J

For coupling capacitor C_1=347 µF operating at 17 V:

- E_{C_1}0.0501 J

The capacitor C o2 can store the most energy among all capacitors due to the highest voltage across it. Balanced energy transfer over every switching cycle at the expense of minimal voltage ripple, and low capacitor stress is seen by almost constant capacitor voltage shapes.

Through overall waveform analysis the cyclic energy transfer is stable between magnetic and electric elements and the switching stress is kept at an adequate level. Besides low ripple and efficient power transfer capabilities the well-behaved inductor current and capacitor voltage shape demonstrate stable closed-loop operation and good dynamic characteristics of the proposed integrated converter topology.

7.8 Chapter Summary

This chapter proposed and provided the simulation evaluation and analysis results of the proposed integrated Buck-Negative Output Super-Lift Luo Converter under various operating conditions. The input and output voltage comparison confirmed that the desired input and output voltage regulation of the converter and steady dual-output operations were obtained. Power analysis was performed to observe the power transfer capability and efficiency utilization of the proposed topology under closed-loop.

The efficiency study presented that the proposed converter has good power conversion ability with less switching loss and efficient utilization of the input source. The switching waveform analysis on the gate, current, and duty ratio of MOSFET as well as inductor current revealed the detail switching behavior of the proposed converter and the dynamic characteristics. The energy analysis of inductor and capacitor indicated the charge/discharge actions used to achieve energy transfer and voltage-lifting operation within the proposed converter. Furthermore, the reference voltage transient analysis exhibited the closed-loop operation and the proper controller functioning under dynamic conditions. In conclusion, the proposed integrated converter system successfully obtains

the regulated dual-output voltage, stable dynamic responses, and acceptable ripple with a satisfying efficiency. These performance metrics make it suitable for application as the auxiliary power source for the EV.

CHAPTER 7

CONCLUSION AND FUTURE SCOPE

In this thesis, the modeling, analysis, and closed-loop control of an integrated dual-output DC-DC converter consisting of a Buck converter and a Negative Output Super-Lift Luo (NOSL-Luo) converter supplied by a single DC input source are described. In this work, the integrated dual output converter is designed to realize positive low voltage and negative high-gain voltage generation simultaneously with decreasing number of separate converter structures, fewer switches and number of controllers.

Both regulated positive low voltage output to feed auxiliary low-power application via Buck converter section and well-regulated negative high-gain voltage output via NOSL-Luo converter section have been successfully generated simultaneously by an integrated Buck and NOSL-Luo converter. By means of two different converter topologies to generate opposite polarity output voltages, it is not required to have an additional converter for negative polarity generation and another one with complicated control structure. The analysis on different switching modes of the integrated circuit demonstrates the operation mechanism and the way the current paths and capacitor charges, discharges take place. The voltage-lift principle of the NOSL-Luo converter is analyzed as well. From the state-space averaging method, the dynamic model is formulated. Based on the model derived, the closed loop transfer functions and PI controller for the entire integrated converter system are designed and simulated. Under different operational conditions, the stability and response of the developed integrated converter is well presented via simulation studies of the startup transient and the step and ripple conditions.

7.1 Major Outcomes of the Proposed Work

The major outcomes obtained from the proposed work are summarized below:

1. Integration of both the Buck and the NOSL-Luo converter topology with a common DC source successfully integrated.
2. Regulation and generation of both positive and negative output voltages is done simultaneously.
3. Reduction in hardware component count and number of switching elements compared to individual converters.
4. Closed loop stable performance under variation of reference voltage input.
5. The controlled inductor ripple current leads to operation in the CCM mode.

6. High-gain negative voltage is generated using voltage-lift operation effectively.
7. Dynamic response is stable and exhibits a reasonable transient performance.
8. Control of the output voltage ripple is maintained and better energy transfer ability.
9. Reasonable efficiency and distribution of power between both the outputs is achieved.
10. Converter performance is verified through simulation and state-space modeling.

7.2 Future Scope

The integrated converter topology can be expanded upon in several other ways to enable practical design and advanced control purposes. Hardware prototypes will be designed in order to provide empirical evidence of the simulation results under practical circumstances. Fuzzy logic control, sliding mode control, model predictive control, intelligent adaptive control and other advanced digital control schemes may be applied so that the transient response is superior and less sensitive to parameter variations. Converter efficiency and switching may be enhanced by employing soft switching and synchronous rectification along with optimized magnetic components design. Moreover, the converter can be bettered to minimize switching stress, reduce EMI and improve converter efficiency using advanced PWM control methods, and efficient layout design techniques. It may also be adapted for a wider range of applications including renewable energy systems, battery management systems, auxiliary power supplies for electric vehicles, communication devices etc that require simultaneous positive and negative unregulated voltage source. Further studies may also be dedicated to enhance the power density, reduce physical size of passive components, and the overall converter reliability, as far as small and powerful power electronic converters are concerned.

REFERENCES

I. V. C. Vennila, K. R. Kumar, S. Padmanaban, and M. S. Bhaskar, "Design of Luo converter with integration of step-down converter," Energy Reports, vol. 12, pp. 4266–4278, 2024.

II. Chen, G., Liu, Y., Qing, X., Ma, M., Lin, Z., 2020. Principle and topology derivation of single-inductor multi-input multi-output dc–dc converters. IEEE Trans. Ind. Electron. 68 (1), 25–36.

III. Faridpak, B., Farrokhifar, M., Nasiri, M., Alahyari, A., Sadoogi, N., 2020. Developing a super-lift luo-converter with integration of buck converters for electric vehicle applications. CSEE J. Power Energy Syst. 7 (4), 811–820.

IV. A. Kumar, R. Ghosh, and S. Padmanaban, "Comprehensive review of topological evolution and control advancements in Luo family converters for electric vehicles," IEEE Access, vol. 11, pp. 1–38, 2023.

V. F. L. Luo and H. Ye, Advanced DC–DC Converters, 2nd ed. Boca Raton, FL, USA: CRC Press, 2016.

VI. R. W. Erickson and D. Maksimović, Fundamentals of Power Electronics, 2nd ed. New York, NY, USA: Springer, 2001.

VII. M. K. Kazimierczuk, Pulse-Width Modulated DC–DC Power Converters, 2nd ed. Hoboken, NJ, USA: Wiley, 2016.

VIII. S. Middlebrook and R. D. Ćuk, "A general unified approach to modelling switching-converter power stages," IEEE Power Electronics Specialists Conference (PESC), pp. 18–34, 1976.

IX. R. D. Middlebrook, "State-space average modelling of switching power converters," IEEE Transactions on Power Electronics, vol. 1, no. 1, pp. 25–32, Jan. 1986.

X. P. Kumar and R. Gupta, "Stability analysis of Luo converter using state space modeling," International Journal of Engineering Research & Technology (IJERT), vol. 3, no. 5, pp. 1021–1026, 2014.

XI. Aden, I.A., Kahveci, H., Şahin, M.E., 2021. Design and implementation of single-input multiple-output dc–dc buck converter for electric vehicles. J. Circuits Syst. Comput.30 , 2150228.

XII. Khalid, H., Mekhilef, S., Mubin, M.B., Seyedmahmoudian, M., Stojcevski, A., Rawa, M. Horan, B., 2022. Analysis and design of series-lc-switch capacitor multistage high gain dc-dc boost converter for electric vehicle applications. Sustainability 14 4495.